JOURNAL OF MORPHOLOGY 248:120–143 (2001)

Evolution and Mechanics of Long Jaws in Butterflyfishes (Family Chaetodontidae)

Lara A. Ferry-Graham,[1]* Peter C. Wainwright,[1] C. Darrin Hulsey,[1] and David R. Bellwood[2]

[1]*Section of Evolution and Ecology, University of California, Davis, California*
[2]*Department of Marine Biology, James Cook University, Townsville, Queensland, Australia*

ABSTRACT We analyzed the functional morphology and evolution of the long jaws found in several butterflyfishes. We used a conservative reanalysis of an existing morphological dataset to generate a phylogeny that guided our selection of seven short- and long-jawed taxa in which to investigate the functional anatomy of the head and jaws: *Chaetodon xanthurus, Prognathodes falcifer* (formerly *Chaetodon falcifer*), *Chelmon rostratus, Heniochus acuminatus, Johnrandallia nigrirostris, Forcipiger flavissimus,* and *F. longirostris.* We used manipulations of fresh, preserved, and cleared and stained specimens to develop mechanical diagrams of how the jaws might be protruded or depressed. Species differed based on the number of joints within the suspensorium. We used high-speed video analysis of five of the seven species (*C. xanthurus, Chel. rostratus, H. acuminatus, F. flavissimus*, and *F. longirostris*) to test our predictions based on the mechanical diagrams: two suspensorial joints should facilitate purely anteriorly directed protrusion of the lower jaw, one joint should allow less anterior protrusion and result in more depression of the lower jaw, and no joints in the suspensorium should constrain the lower jaw to simple ventral rotation around the jaw joint, as seen in generalized perciform fishes. We found that the longest-jawed species, *F. longirostris*, was able to protrude its jaws in a predominantly anterior direction and further than any other species. This was achieved with little input from cranial elevation, the principal input for other known lower jaw protruders, and is hypothesized to be facilitated by separate modifications to the sternohyoideus mechanism and to the adductor arcus palatini muscle. In *F. longirostris* the adductor arcus palatini muscle has fibers oriented anteroposteriorly rather than medial-laterally, as seen in most other perciforms and in the other butterflyfish studied. These fibers are oriented such that they could rotate the ventral portion of the quadrate anteriorly, thus projecting the lower jaw anteriorly. The intermediate species lack modification of the adductor arcus palatini and do not protrude their jaws as far (in the case of *F. flavissimus*) or in a purely anterior fashion (in the case of *Chel. rostratus*). The short-jawed species both exhibit only ventral rotation of the lower jaw, despite the fact that *H. acuminatus* is closely related to *Forcipiger*. J. Morphol. 248:120–143, 2001.

KEY WORDS: lower jaw protrusion; mobile suspensorium; mechanics; prey capture; morphology; function

Morphological novelties are of interest in both ecological and evolutionary contexts as they tend to challenge our ideas about how organisms work from a mechanical standpoint and the limits to change from a functional point of view. Some butterflyfishes in the family Chaetodontidae have an exceptionally elongate premaxilla and mandible (lower jaw) relative to other perciform fishes. Elongate jaws are fairly widespread in the family Chaetodontidae, occurring in all members of the genera *Forcipiger, Chelmon*, and *Chelmonops*. Slightly elongate jaws are also found in some members of *Prognathodes* and even some *Chaetodon*. Thus, some form of jaw elongation is found in half of the recognized genera of Chaetodontidae (sensu Blum, 1988; Fig. 1). However, we actually know little about how the peculiar trait of elongate jaws arose, or how elongate jaws function.

The evolution and mechanics of short-jawed butterflyfishes have been studied fairly extensively (Motta, 1982, 1984a,b, 1985, 1988, 1989). Butterflyfishes typically have short, robust jaws that are used for biting corals and other attached prey, as this is the most common feeding mode in the family (Harmelin-Vivien and Bouchon-Navaro, 1983; Sano, 1989). The jaw mechanics associated with this feeding mode have been described (Motta, 1985, 1989), as have the associated foraging behaviors (e.g., Harmelin-Vivien and Bouchon-Navaro, 1983; Tricas, 1989; Cox, 1994). Zooplanktivores are less common within the butterflyfishes, but short-jawed species have also been studied in the context of how their jaws function to capture mid-water prey (Motta, 1982, 1984b). Corallivorous species have presumably retained a robust jaw, and often strong teeth, from a biting ancestor. Some zooplanktivo-

Contract grant sponsor: NSF; Contract grant number: IBN-9306672; Contract grant sponsor: the Australian Research Council.

*Correspondence to: Lara A. Ferry-Graham, Section of Evolution and Ecology, University of California, Davis, CA 95616.
E-mail: laferry@ucdavis.edu

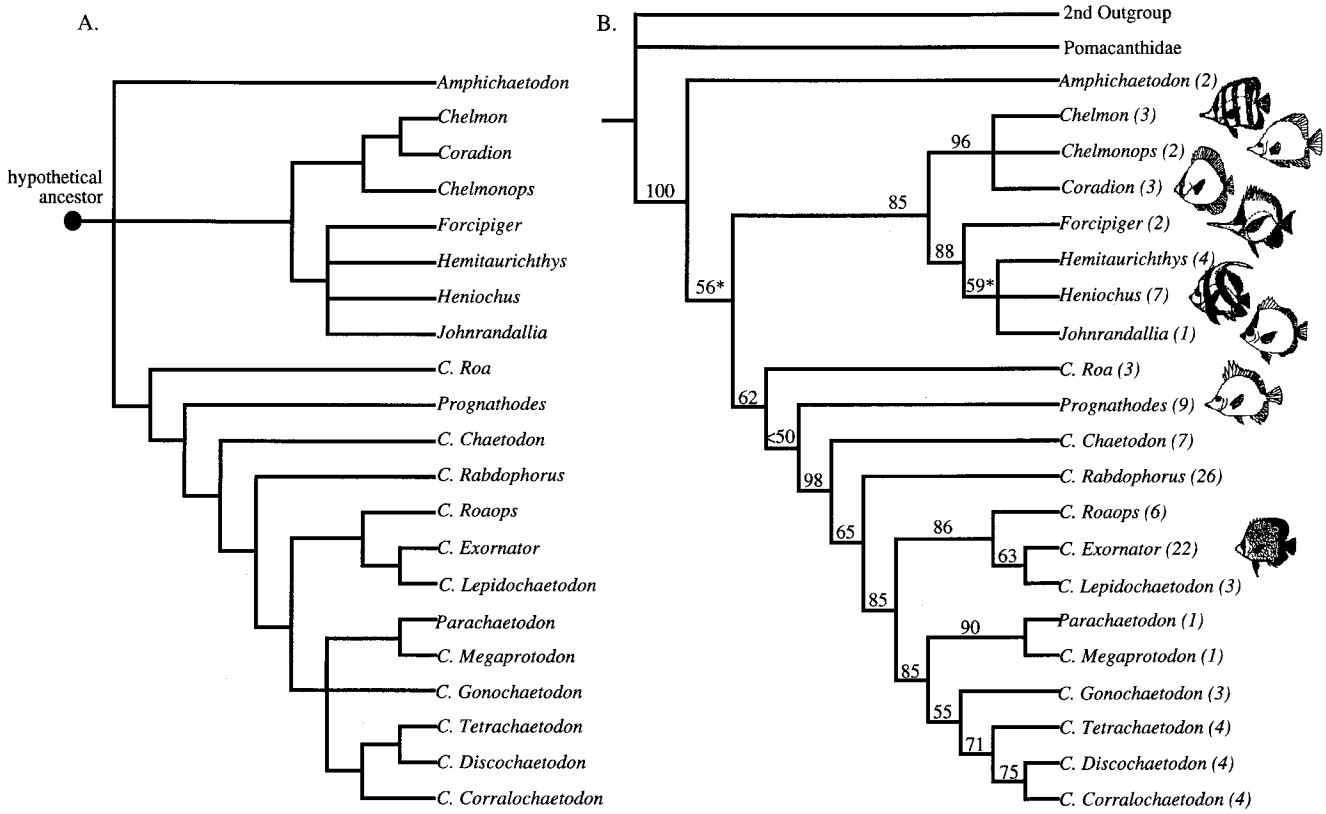

Fig. 1. Phylogeny of the chaetodontid fishes. Shown is Blum's (1988) strict-consensus tree (**A**) and our revised phylogeny based on a conservative recoding of Blum's (1988) morphological character data (**B**). The strict-consensus tree and bootstrap tree agreed except for two nodes. Shown in **B** is the strict-consensus tree with the addition of the two nodes that were resolved in the bootstrap tree, which are indicated by asterisks (the bootstrap values for all nodes are given). In the strict-consensus tree these two resolved nodes were a tritomy in the case of *Amphichaetodon* + the *Forcipiger* and *Chelmon* clade + all other butterflyfishes (bootstrap value placing *Amphichaetodon* ancestral to the other two clades = 56%) and a quadritomy in the case of *Forcipiger* + *Hemitaurichthys* + *Heniochus* + *Johnrandallia* (bootstrap value placing *Forcipiger* ancestral to the other three genera = 59%). For historical accuracy we have retained the nomenclature chosen by Blum (1988) as much as possible for the terminal taxonomic units. For reference, in his original trees Blum (1988) elevated *Roa, Chaetodon, Rabdophorus, Roaps, Exornator, Lepidochaetodon, Megaprotodon, Gonochaetodon, Tetrachaetodon, Discochaetodon, Corallochaetodon* (which contains *Citharodeus*; see Appendix A) to the generic status but all are currently considered subgenera of *Chaetodon* (Allen et al., 1998), so we refer to them as such in the trees shown here with the initial *C* before each name. Despite its placement on the phylogeny, *Parachaetodon* is still afforded generic status. *Prognathodes* has been elevated to generic status since Blum's work (Allen et al., 1998). Allen et al. (1998) published the most recent publication on butterflyfishes and did not recognize *C. Roaops* and *C. Exornator*. Allen et al. (1998) also retained *C. Rhombochaetodon* and *C. Chaetodontops*. Blum (1988) subsumed *C. Rhombochaetodon* in *C. Exornator*. Nalbant, 1971, placed *C. Chaetodontops* within *C. Rabdophorus* (a subgenus recognized by both authors), and *C. Roaops* Mauge and Bauchot 1984 contains all of the previous members of *C. Roa* except the type specimen. The number of species in each genus/subgenus is indicated in parentheses (after Blum, 1988). Icons are shown for select genera in each clade, demonstrating the diversity of jaw length (the jaw of each icon points to its respective name on the phylogeny). Icons are modified after Allen et al. (1998).

rous species have secondarily lost some of these features; however, species often employ behavioral modifications to utilize novel prey (Motta, 1988, 1989). In both cases, the feeding mechanism largely resembles the generalized perciform condition in basic mechanical movements.

However, in the case of species like *Forcipiger longirostris*, which possesses exceptionally elongate jaws, radical modifications have occurred to the feeding mechanism. Common names assigned within the general literature, such as forceps fish (see, for example, Randall, 1985; Randall et al., 1990), suggest a function of the elongate jaws similar to how biting short jaws might work, except that the jaws are longer. However, there is additional evidence that long-jawed butterflyfishes are capable of modified feeding kinematics (Motta, 1988, 1989; Ferry-Graham et al., in review). Motta (1988) noted rotation of the suspensorium during feeding in both *Forcipiger* species. During feeding both the upper and lower jaws are protruded anteriorly.

Protrusion of the lower jaw is unusual in teleosts. The only other description of anteriorly directed protrusion of the lower jaw is for the "sling jaw" wrasse *Epibulus insidiator* that possesses a novel joint within the suspensorium that facilitates anterior translation of the jaw joint, and hence extensive jaw protrusion (Westneat and Wainwright, 1989; West-

neat, 1990). Most fishes protrude only the upper jaw (premaxilla) when they feed and the ability of teleost fishes to protrude their upper jaw is thought to be a major contributing factor to the success and radiation of the perciform fishes (Schaeffer and Rosen, 1961; Alexander, 1967; Lauder, 1982, 1983; Motta, 1984a). The lower jaw is typically depressed, rather than protruded, by rotating ventrally and anteriorly about the posteriorly positioned jaw joint located on the suspensorium at the quadrate.

In this study, we extend a previous analysis of butterflyfish relationships (Blum, 1988). We used a revised phylogeny to make informed selections of taxa for a comparative study across levels of morphological modification. As a first step towards understanding the function of the long jaws in butterflyfishes, we studied the anatomy of long-jawed species and short-jawed species from each of the major clades. From these observations of jaw linkage mechanics we developed simple mechanical diagrams of how the jaws are protruded in each species. We then compared quantitative kinematic data obtained from high-speed video of five of these species feeding on planktonic prey with the qualitative predictions from the diagrams. We used these together to gain insight into how the long jaws function in prey capture.

MATERIALS AND METHODS

Phylogeny of the Chaetodontidae

We reanalyzed a modified morphological data matrix of 34 characters coded for 21 phenetically distinct and putatively monophyletic groups in the Chaetodontidae (Blum, 1988). These 21 morphologically distinct groups, used as the operational taxonomic units (OTUs) in this analysis, were designated by Blum (1988) after he examined specimens or radiographs of 86 of the approximately 120 species of Chaetodontidae. Each morphologically distinct group was found to be qualitatively identical with respect to the morphological characters examined, and these groups largely reflect existing taxonomic designations of genera as well as previously designated subgenera within the genus *Chaetodon*. However, on examining the morphology Blum (1988) moved several of the species within the genus *Chaetodon* into OTUs that do not reflect their widely accepted subgeneric classifications (See Appendix A). Using his groups, the first objective of our reexamination was to reconstruct the most parsimonious interrelationships of the groups using a revised matrix and thereby test the robustness of Blum's (1988) original evolutionary hypothesis to a different coding of characters. The second objective was to provide bootstrap support for the proposed relationships of the 21 groups within the Chaetodontidae.

Blum's phylogenetic trees were based on highly ordered character data that we believed had the potential to exert a strong influence on the phylogenetic relationships constructed (Fig. 1A). Character ordering imposes differential costs on the way characters are optimized on the tree (Mayden and Wiley, 1992). The ordering of morphological characters imposes specific hypotheses about the way in which morphological evolution occurred and could lead to circularity since character ordering can predetermine the inferences of the evolutionary relationships under investigation (Swofford and Maddison, 1992). Nine of the 34 characters used in the production of Blum's (1988) phylogenetic hypothesis were coded as multistate and ordered: five characters had three ordered states, two characters had four states, one character had five ordered states, and one character in Blum's matrix was coded as having eight ordered character states. Because of the significant proportion of characters originally treated as ordered, and the large number of states proposed for several of these characters, we explored the consequences of a different character matrix and recoded all previously ordered multistate characters as unordered (Appendix B).

We also eliminated all unknown character states from the original matrix to increase character resolution and to avoid any problems associated with missing characters (Maddison, 1993). Three cells had previously been coded as unknown because the original phylogenetic analysis combined the two outgroups, Pomacanthidae and a second outgroup composed of the Ephippidae, Scatophagidae, and Acanthuroidei, and the genus *Drepane*, into a single hypothetical ancestor (Blum, 1988). We separated the hypothetical ancestor into two distinct outgroups. This separation increased resolution in three characters in which the two outgroups displayed different character states (Appendix B, characters 21, 26, 29). In addition, we changed the coding of three character states within ingroup taxa that were originally treated as too ambiguous to code (Appendix B, characters 2, 15, 22). *Parachaetodon* exhibits uniquely derived predorsal bones and a derived origin of the palato-palatine ligament. The genus *Forcipiger* exhibits novel jaw and tooth morphology according to Blum's character coding. These unique character states all occurred in characters which were treated as ordered in Blum's analysis. Because of their uniquely derived condition, they were likely difficult to place in an ordered transformation series. The three character states were recoded from unknown to apomorphic conditions for the taxa exhibiting them.

A maximum parsimony analysis of all taxa was conducted with Swofford's (1993) PAUP computer package using the branch-and-bound algorithm to find all most-parsimonious trees. Bootstrap analyses were performed on these data with PAUP using 100 replicates and tree bisection and reconnection (TBR) branch swapping. Because we were interested in the evolution of novel feeding morphology in the long-jawed species, we also analyzed relationships

TABLE 1. Source and details regarding specimens used for analysis

Species	Source	Region of collection	N			Measurements	
			Total examined	Cleared & stained*	Kinematic analysis	TL; OTL	Jaw:Head length
Forcipiger							
longirostris	CC1 (live)	Great Barrier Reef	5	2	3	11.2–14.9; 8.2–11.6	0.90
flavissimus	CD1 (live)	Hawaii	10	3	3	11.3–12.2; 8.2–8.8	0.74
Heniochus							
acuminatus	CD2 (live)	Indonesia	3	1	3	6.2–9.8; 5.4–9.0	0.45
singularis	CD1 (live)	Philippines	1	1		5.9; 5.2	0.48
chrysostomus	CD1 (live)	Philippines	1	1		6.8; 6.0	0.41
Johnrandallia							
nigrirostris	AQ1 (frozen)	Sea of Cortez	3	1		4.4–5.3; 3.8–4.8	0.46
Chelmon							
rostratus	CD2 (live)	Indonesia	6		3	9.9–10.7; 8.0–8.7	0.64
	CD1 (live)	Philippines	5	3		4.2–10.7; 3.4–8.7	
Prognathodes							
falcifer	AQ1 (frozen)	San Diego, CA, USA	3	1		15.2–16.2; 13.2–14.2	0.52
aculeatus	RD1 (live)	Florida	2	2		5.4–7.1; 4.6–5.9	0.52
Chaetodon							
xanthurus	CD1 (live)	Philippines	3	1	3	6.6–7.4; 6.0–6.6	0.49
auriga	CC2 (live)	Indonesia	2	1		6.8–7.8; 6.1–7.2	0.41
striatus	WC (dead)	Bahamas	2	1		15.8–16.2; 14.2–14.6	0.47

CC1 = commercial collector, Cairns, Australia; RD1 = retail distributor, Sacramento, California, USA; CD1 = commercial distributor, Sacramento, California, USA; AQ1 = Birch Aquarium, University of California San Diego, USA; CD2 = commercial distributor, Los Angeles, California, USA; WC = wild caught/killed using a pole spear and scuba.
TL = total length; cm; OTL = anterior margin of orbit to tail tip; cm.
Jaw: head length = ratio of mandible length to head length from posterior margin of opercle to anterior tip of premaxilla; not elongate, <0.50; slightly elongate, 0.50–0.59; moderately elongate, 0.60–0.79; and highly elongate, ≥ 0.80.
*The number of cleared and stained specimens is a subset of the total number examined. Where possible, the same specimens were not used for both clearing and staining and the kinematic analysis.

among the taxa with several characters removed from the character matrix. We removed characters that are generally believed to be intimately associated with the feeding apparatus of perciform fishes, including characters 10, 15, 16, 21, 22, 23, 24, and 25 (see Appendix B). We then conducted a second parsimony analysis to test how much the structure of the tree depended on these characters and compared the tree to the "total evidence tree," the tree constructed using all of the available characters.

Gross Morphology and Linkage Models

To examine the morphology of the elongate jaws and how they differed from the jaws of other butterflyfishes, we studied seven species: *Chaetodon xanthurus, Prognathodes falcifer* (formerly *Chaetodon falcifer*), *Chelmon rostratus, Heniochus acuminatus, Johnrandallia nigrirostris, Forcipiger flavissimus,* and *F. longirostris*. We used the phylogeny to inform our selection of these species; thus, some preliminary phylogenetic results must be mentioned here. Throughout the article we will discuss them in decreasing order of their phylogenetic distance from the highly morphologically modified genus, *Forcipiger* (see Fig. 1B). Each vary in jaw length and we categorized them based on the relative length of the jaw (see Table 1). As jaw length also influenced our selection of taxa, these preliminary results will be presented here with our species descriptions. The species are similar in diet and habit in that none are coral biters and all utilize relatively soft, benthic invertebrate prey in varying proportions (see review in Ferry-Graham et al., 2001).

We studied *Chaetodon xanthurus* (subgenus *Exornator*; Fig. 1B) as the basis of our comparison with all other chaetodontids studied. This species is considered short-jawed (Table 1). We also examined individuals of *C. striatus* (subgenus *Chaetodon*) and *C. auriga* (subgenus *Rabdophorus*) to determine the generality of our observations regarding *Chaetodon* anatomy (Table 1). We also obtained specimens of the slightly long-jawed *Prognathodes falcifer*, which was previously included with the genus *Chaetodon* (Blum, 1988), as well as two *P. aculeatus* for comparison (Table 1).

We included *Chelmon rostratus* in our analysis as well. This species is a member of the putative sister clade to the *Forcipiger* clade (the *Chelmon* clade: *Chelmon* + *Chelmonops* + *Coradion*; Fig. 1B), and has moderately elongate jaws (Table 1). Note that moderately elongate jaws are also reported in *Chelmonops* within this clade. *Chelmon rostratus* has been observed probing its jaws into crevices on the reef to procure invertebrate prey (Allen et al., 1998).

Heniochus and *Johnrandallia* are within the *Forcipiger* clade (Fig. 1B; *Forcipiger* + *Hemitaurichthys* + *Heniochus* + *Johnrandallia*) but possess short jaws (Table 1), as does *Hemitaurichthys* in this clade. We studied *Heniochus acuminatus* and also

examined single individuals of *H. singularis* and *H. chrystostomus* to determine the generality of our findings regarding the genus. *Johnrandallia nigrirostris* is the only member of the genus *Johnrandallia* and was studied to determine the generality of our findings regarding the *Forcipiger* clade. In comparison with the other species studied here, *H. acuminatus* takes the largest proportion of midwater prey (see review in Ferry-Graham et al., submitted). *Johnrandallia nigrirostris* is known to clean parasites off other fishes in addition to a diet of benthic invertebrates (Allen et al., 1998).

Forcipiger longirostris has the longest jaws known of any butterflyfish (Motta, 1984b; Table 1). *Forcipiger flavissimus* is the only other member of the *Forcipiger* genus and has moderately elongate jaws (Table 1). We studied both Forcipiger species to accurately characterize the genus. Note that *Forcipiger longirostris* feeds almost entirely on small caridean shrimp, the most elusive prey of any of the species studied. *Forcipiger flavissimus* takes a more diverse range of mobile and attached prey, including polychaete setae and urchin tube feet (see review in Ferry-Graham et al., submitted). Both have been observed probing their snouts into cracks and crevices on the reef (P.J. Motta, personal communication). However, recent work has also refuted the notion that the elongate jaws facilitate extreme suction feeding (Ferry-Graham et al., submitted).

In each of the species the morphology was investigated in fresh specimens (anesthetized or recently deceased) or frozen specimens, and specimens fixed in formalin and stored in 70% ethanol. Muscle origins, insertions, and fiber arrangements were determined from preserved specimen dissection. Specimens were cleared using trypsin and double-stained using an Alcian-blue cartilage stain and alizarin-red bone stain (Dinkerhus and Uhler, 1977). The cranial skeletal anatomy of each of the primary species was drawn from cleared and stained specimens with the aid of a camera lucida. Movements of joints associated with jaw motion were determined through direct manipulation of anesthetized, thawed, and cleared and stained specimens. This combination of information was used to construct mechanical diagrams of jaw function.

Kinematic Analysis

We obtained high-speed video footage of prey capture from *Chaetodon xanthurus, Chelmon rostratus, Heniochus acuminatus, Forcipiger flavissimus*, and *F. longirostris* (Table 1). All species were filmed feeding on live brine shrimp (*Artemia* sp.). *Forcipiger flavissimus, Chel. rostratus, H. acuminatus*, and *C. xanthurus* were housed at 27 ± 2°C in 100-L aquaria at the University of California, Davis. Video sequences were obtained with an NAC Memrecam ci digital video system recording at 250 images s^{-1} (*F. flavissimus*) or 500 images s^{-1} (*Chel. rostratus, H. acuminatus*, and *C. xanthurus*). *Forcipiger longirostris* were maintained at 23 ± 2°C in 100-L aquaria at James Cook University in Townsville, Australia. Feeding sequences of this species were recorded at 300 or 500 images s^{-1} with an Adaptive Optics Kineview digital video system. Frame rates were selected so that at least 20 frames per feeding sequence were obtained. The tanks were illuminated with two 600W floodlights to enhance image clarity. For precise scaling during analysis, a rule was placed in the field of view and recorded for several frames. Fish were offered prey one or a few items at a time and allowed to feed until satiated. Filming generally occurred over a 2–3-day period for each individual.

We analyzed only sequences in which a lateral view of the fish could clearly be seen in the image and the fish was perpendicular to the camera to prevent measurement error. Since several of the species filmed here routinely hold the mouth slightly ajar and do not increase the gape to capture prey (see Ferry-Graham et al., submitted), time zero (t_0) for feeding trials was taken as the first image that movement of the jaws in a ventral or anterior direction was detected. Sequences ended at the conclusion of the strike as indicated by the return of the jaw to the relaxed, prefeeding position. Four feeding sequences were analyzed from each individual of each of the five species.

To quantify movement of skeletal elements related to protrusion of the lower jaw we digitized points on the video frames and calculated several kinematic variables from the points. The following points were digitized in each video frame of each sequence using NIH Image 1.6 for Macintosh or Didge for PC (A. Cullum, University of California Irvine; Fig. 2): 1) the anterior tip of the premaxilla; 2) the dorsalmost anterior margin of the maxilla; 3) the posterior margin of the nasal bone; 4) the dorsalmost tip of the neurocranium as approximated by external morphology; 5) the dorsalmost tip of the preopercle; 6) the posteriormost margin of the opercle; 7) the dorsal margin of the insertion of the pectoral fin on the body (a reference point); 8) the anteroventral tip of the preopercle; 9) the ventral tip of the maxilla; and 10) the anterior tip of the lower jaw (dentary). The angles calculated from these digitized points included (see Fig. 2C): a) the angle of the neurocranium relative to the body (cranial elevation); b) the angle of the preopercle with the neurocranium; c) the angle of the preopercle with the lower jaw; and d) the angle of the maxilla with the premaxilla (maxilla rotation; all measured in degrees). The quadrate cannot be seen externally and therefore could not be digitized directly. But, the preopercle is attached by ligaments along its anterior margin to the posterior edge of the quadrate and was therefore constrained to follow the same path of motion. Changes in the angle of the preopercle with the neurocranium and the lower jaw (angles b and c), which indicated the degree of rotation of the

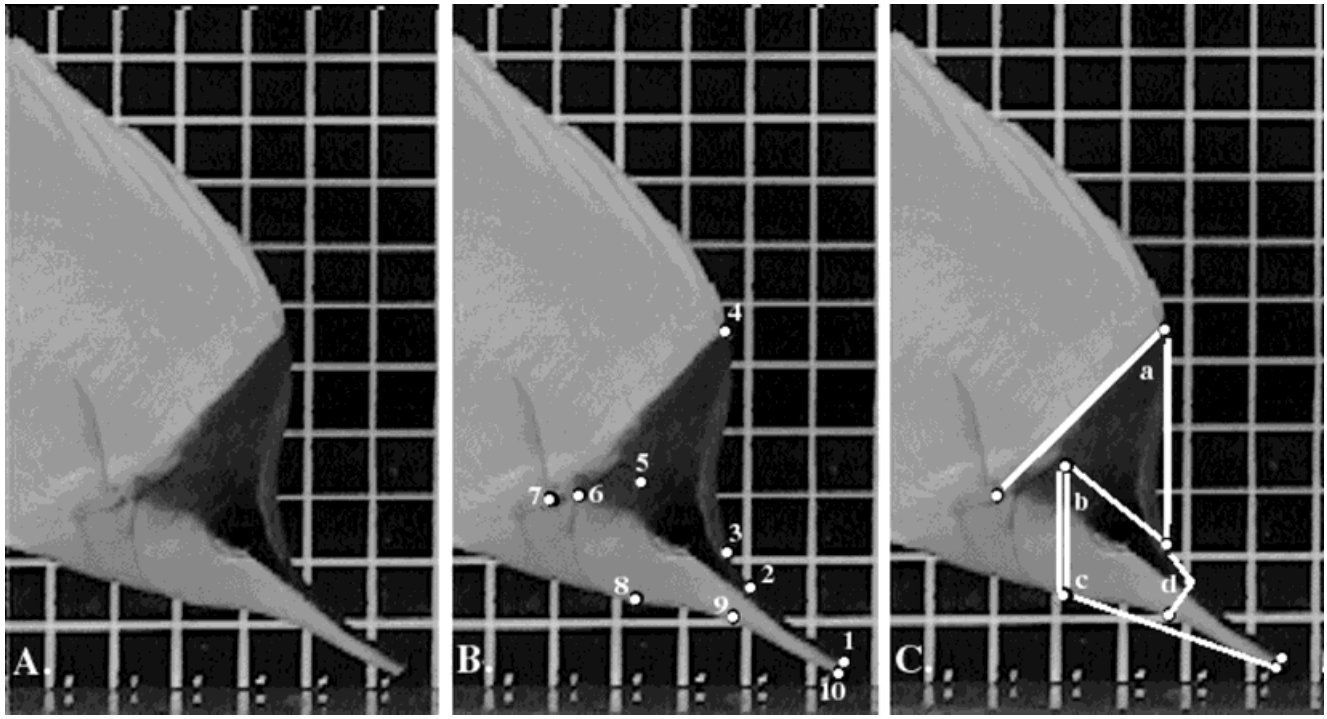

Fig. 2. Digitizing protocol for calculating displacements and angles achieved during prey capture: **A**: A sample image of *Forcipiger flavissimus* from the NACci high-speed video camera. **B**: The points used to measure the path of the lower jaw and used to determine the angles of the preopercle with the lower jaw and the neurocranium. **C**: Angles that were measured. Numbered points in frame **B** correspond to descriptions of the points digitized in the methods section of the text. Letters in frame **C** correspond to angular variables (see also Methods): a) cranial elevation, b) angle of the preopercle with the neurocranium, c) angle of the preopercle with the lower jaw, and d) maxilla rotation.

preopercle during prey capture, were measured as proxies for rotation of the quadrate on the hyomandibula (angle b), and rotation of the lower jaw on the quadrate (angle c).

The four angular variables (a–d above) were simultaneously compared among species using MANOVA (Statview v. 4.5). Given a significant MANOVA, post-hoc univariate ANOVA was performed on each of the four variables. If the ANOVA was significant, a Fisher's paired least significant difference post-hoc test was used to determine which species were different from one another. A single ANOVA was used to compare the displacement variable of maximum dentary protrusion among species followed by a Fisher's PLSD post-hoc test. Absolute displacement, rather than standardized, was used in the ANOVA.

RESULTS

Phylogeny

The revised character matrix gave 10 equally most-parsimonious trees each with 83 steps. Like Blum's original strict consensus tree (Fig. 1A), our analysis separated all taxa in Chaetodontidae into three primary groups (Fig. 1B): 1) a clade containing the genus *Amphichaetodon*; 2) a clade containing the groups *Chelmonops, Chelmon, Coradion, Forcipiger, Hemitaurichthys, Heniochus*, and *Johnrandalia*; and 3) a clade containing the taxa included in the group *Chaetodon, C. Roa, Prognathodes*. The strict consensus tree produced in this analysis differed in topology from Blum's (1988) tree in two primary ways (Fig. 1B). First, in Blum's tree the group *C. Gonochaetodon* formed a trichotomy with the group *Parachaetodon* + *C. Megaprotodon* and the group *C. Tetrachaetodon* + *C. Discochaetodon* + *C. Corallochaetodon*. In our phylogeny *C. Gonochaetodon* was found to be the sister group to *C. Tetrachaetodon* + *C. Discochaetodon* + *C. Corallochaetodon*, and this group of four taxa was found to be the sister group to *Parachaetodon* + *C. Megaprotodon*. Second, *Chelmonops*, which differed in Blum's matrix by only a single ordered character state from the clade *Chelmon* + *Chelmonops*, in our analysis formed a polytomy with the other two genera in our strict consensus tree.

The monophyly of the clade containing *Chelmonops, Chelmon*, and *Coradion*, as well as the monophyly of the clade composed of the four taxa *Forcipiger, Hemitaurichthys, Heniochus*, and *Johnrandalia* both had strong bootstrap support (>96% and >88%, respectively; Fig. 1B). *Chelmon, Chelmonops,* and *Coradion* all shared the derived features

of having only five branchiostegal rays (character 9), a novel epibranchial shape (character 13), and different predorsal bone anatomy (character 2). The clade of four taxa containing *Forcipiger* was supported by unique features of the kidney (character 8) and the shape of the medial extrascapular (character 30). Although support was weak, there was some tentative evidence for *Forcipiger* (>59% bootstrap support) being placed as the sister taxon to a clade containing *Hemitaurichthys, Heniochus*, and *Johnrandalia*. Furthermore, the monophyly of a clade uniting the seven taxa in these two clades, which contain the Chaetodontidae species with the longest jaws, had >85% bootstrap support. The shape of the dorsal hypohyal, the shape of the first epibranchial, the fact that the ethmoid foramen is not enclosed in the lateral ethmoid, and the insertion of the vertical palato-vomerine ligament onto the maxillary process (characters 12, 13, 17, and 23) all represent synapomorphies which support the monophyly of this group of seven taxa. The groups *C. Roa* and *Prognathodes* are moderately supported sister groups to what has been considered the large genus *Chaetodon*. The clade containing the rest of the taxa in the family Chaetodontidae is the strongest supported clade on the tree (98% bootstrap support). The arrangement of the predorsal bones, the presence of anterior diverticulae on the swimbladder, the absence of vertical ridges on the anterior mesethmoid, the reduction of the parietal dorsoventrally, and because the lateral escapular does not enclose the temporal canal (characters 2, 6, 20, 28, and 29, respectively) are all diagnostic of this clade.

The elimination of the eight characters intimately related to the feeding morphology reduced the number of ingroup taxa in the analysis to 18. The group *Chelmonops, Chelmon*, and *Coradion* collapsed, as did two subgenera of *Chaetodon, C. Gonochaetodon* + *C. Tetrachaetodon,* leaving only two total groups in place of the five. The parsimony analysis produced a tree with 48 steps. The majority of the tree topology that was recovered with all 34 characters was recovered intact in this reduced character analysis. However, there were two differences in the topology. There was a loss of resolution between the above *C. Gonochaetodon* pair, *C. Discochaetodon*, and *C. Corallochaetodon*. In addition, *Johnrandallia* came out as the outgroup to *Heniochus, Hemitaurichthys,* and *Forcipiger*. This difference in placement of *Forcipiger* is central to an understanding of the evolution of the mobile suspensorium and elongate jaws within this group. The remaining tree topology mirrored that of the analysis containing all 34 characters.

Gross Morphology

The features of the skull and jaws that appear to be important in functionally distinguishing *Chaetodon* from the other taxa studied are related to the suspensorial elements and their associated ligamentous connections. Most important of these are the palatine, the hyomandibula, the symplectic, and the quadrate, endo-, ecto-, and metapterygoids (Fig. 3). A ligament we will refer to as the ethmopalatoendopterygoid ligament is robust in *Chaetodon* and passes in two halves from the lateral ethmoid to the endopterygoid and from the lateral ethmoid to the palatine (Fig. 4). The latter portion of this ligament has been referred to as the posterior ventromedial palatine ligament (Blum, 1988). The lateral ethmoid contacts both the palatine and the endopterygoid and appears to be held by short, ligamentous connections. The palatine and endopterygoid are fused via a bony suture and no anterior motion of the palatine is detectable during jaw movement. There is also a vertical vomeropalatine ligament that extends from the anterior process of the palatine ventrally to the lateral surface of the vomer (sensu Blum, 1988; Fig. 4). The suspensorium is immobile in the dorsoventral plane, as seen in the generalized perciform condition, and during jaw manipulation in cleared and stained specimens the premaxilla is protruded while the lower jaw rotates ventrally. *Prognathodes* shares these features with *Chaetodon* (Figs. 3, 4).

In *Chelmon rostratus* the suspensorial bones are slightly reduced relative to *Chaetodon* (Fig. 5). The palatine and endopterygoid are not fused; the medial surface of the palatine is attached to the lateral surface of the endopterygoid via a ligament that we refer to as the palatoendopterygoid ligament (Fig. 6). A flange on the palatine passes deep into the ectopterygoid, limiting rotation of the palatine at this soft connection. There is also a ligament that extends from the lateral ethmoid to the palatine (Fig. 6). This appears to be a modification of the ethmopalatoendopterygoid ligament; one segment of the robust, two-part ligament found in *Chaetodon*. Unique to *Chel. rostratus* is the configuration of the vertical vomeropalatine ligament; a few thin fibers appear to extend ventrally from the anterior projection of the palatine deep into the facia of the adductor mandibulae muscle (Fig. 6). A posterior joint within the suspensorium is present between the proximal head of the hyomandibula and the neurocranium. This joint is present in nearly all teleost fishes (Winterbottom, 1974), but it is modified in *Chel. rostratus* to permit motion in an anterior–posterior direction. In *Chel. rostratus* limited anterior rotation of the hyomandibula on the neurocranium is permitted because of the mobile connection between the endopterygoid and the palatine, allowing the endopterygoid to slide under the palatine. The hyomandibula is able to rotate forward by about 5°, along with the quadrate, symplectic, endo-, ecto-, and metapterygoid complex. This rotates the jaw joint (quadrate-articular) anteriorly, allowing the lower jaw to be protruded while also being depressed in manipulated specimens.

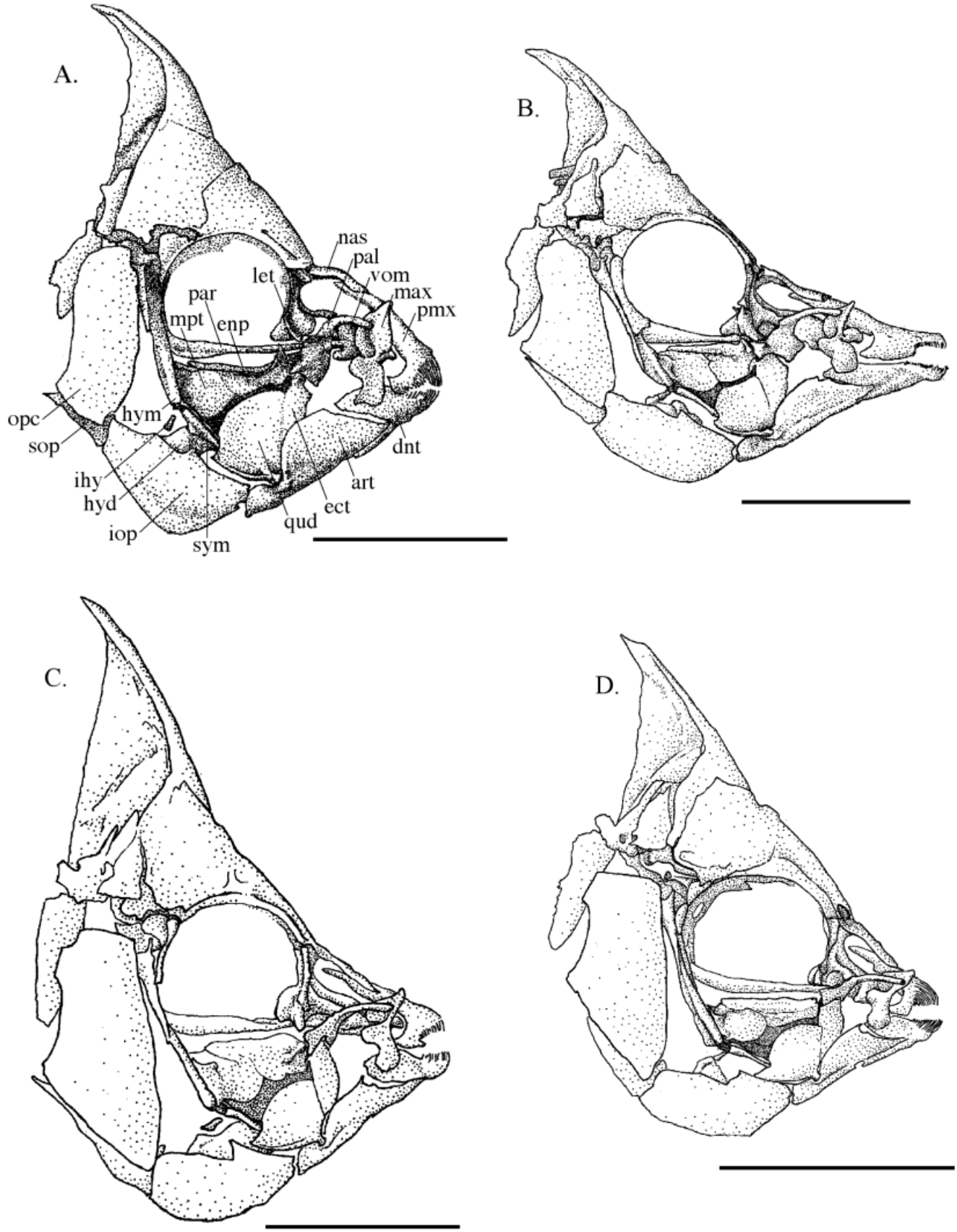

Fig. 3. Cranial anatomy of butterflyfishes drawn from cleared and stained specimens. **A**: *Chaetodon xanthurus*. **B**: *Prognathodes falcifer*. **C**: *Heniochus acuminatus*. **D**: *Johnrandallia nigrirostris*. The orbital bones have been cut near the neurocranium and removed and the preopercle has been removed to facilitate a view of the suspensorial elements. opc, opercle; sop, subopercle; hym, hyomandibula; ihy, interhyal, hyd, hyoid; mtp, metapterygoid; enp, endopterygoid; ect, ectopterygoid; qud, quadrate; sym, symplectic; iop, interopercle; par, parietal; let, lateral ethmoid; pal, palatine; nas, nasal bone; vom, vomer; max, maxilla; pmx, premaxilla; art, articular; dnt, dentary (articular + dentary = mandible or lower jaw). Scale bars are 1.0 cm.

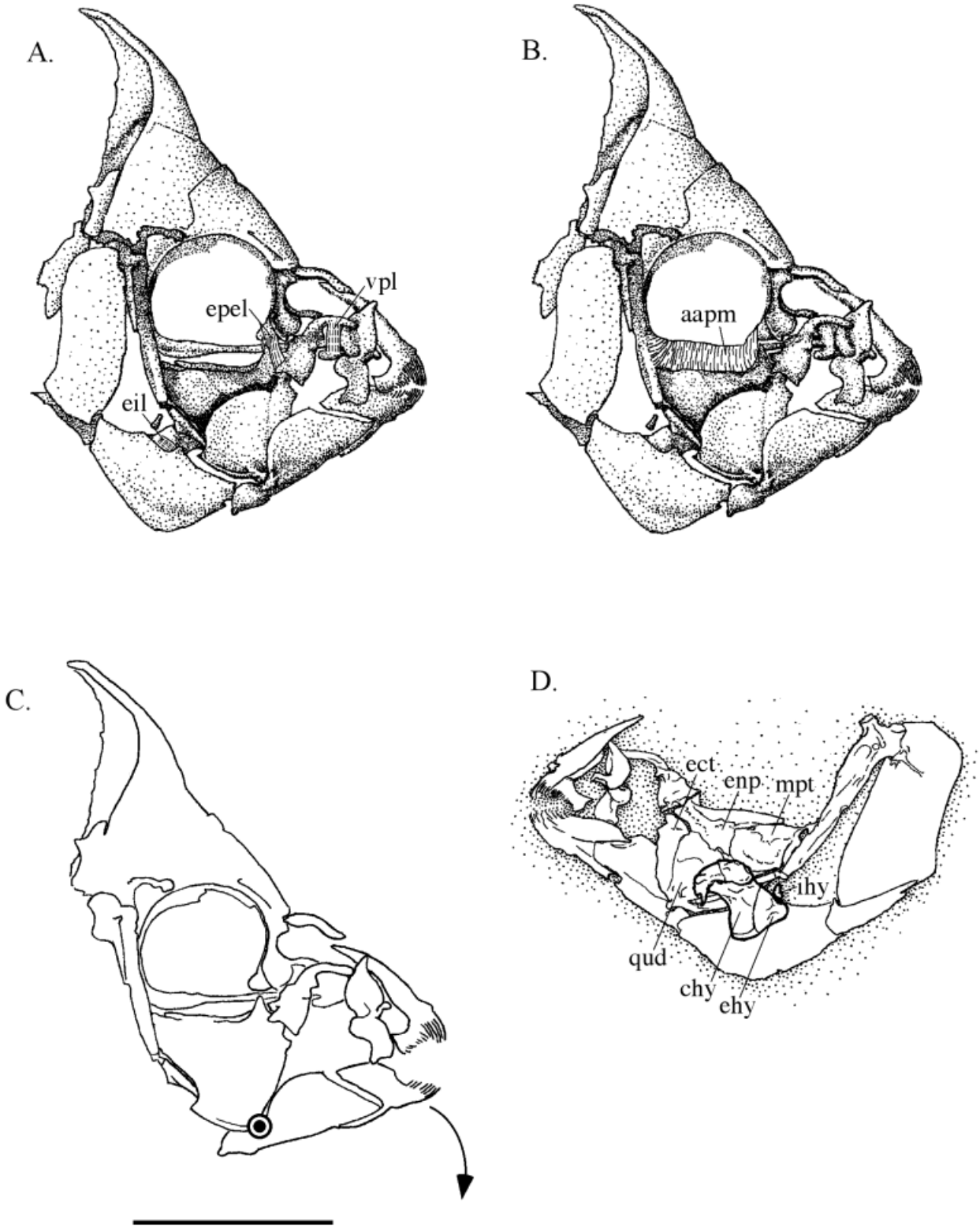

Fig. 4. Specific aspects of the cranial anatomy of *Chaetodon xanthurus.* **A**: Ligaments associated with the suspensorium. **B**: The superficial portion of the adductor arcus palatini muscle. **C**: Reduced cranial morphology illustrating jaw motion with one joint at the lower jaw. **D**: Reduced cranial morphology showing a medial view of the hyoid apparatus on the same side of the head (note that stippling has been used to enhance the sections where bones are not present). eil, epihyal-interopercular ligament; epel, two-part ethmopalatoendopterygoid ligament; vpl, vomeropalatine ligament; aapm, adductor arcus palatini muscle; ehy, epihyal; chy, ceratohyal (epihyal + ceratohyal = hyoid in Fig. 3); ihy, interhyal, ect, ectopterygoid; enp, endopterygoid; mtp, metapterygoid; qud, quadrate. The fiber orientation of the adductor arcus palatini muscle is indicated by the solid lines in each diagram. In the mechanical drawing rotating joints are indicated by points and the direction of movement is indicated by arrows. Scale bars are 1.0 cm.

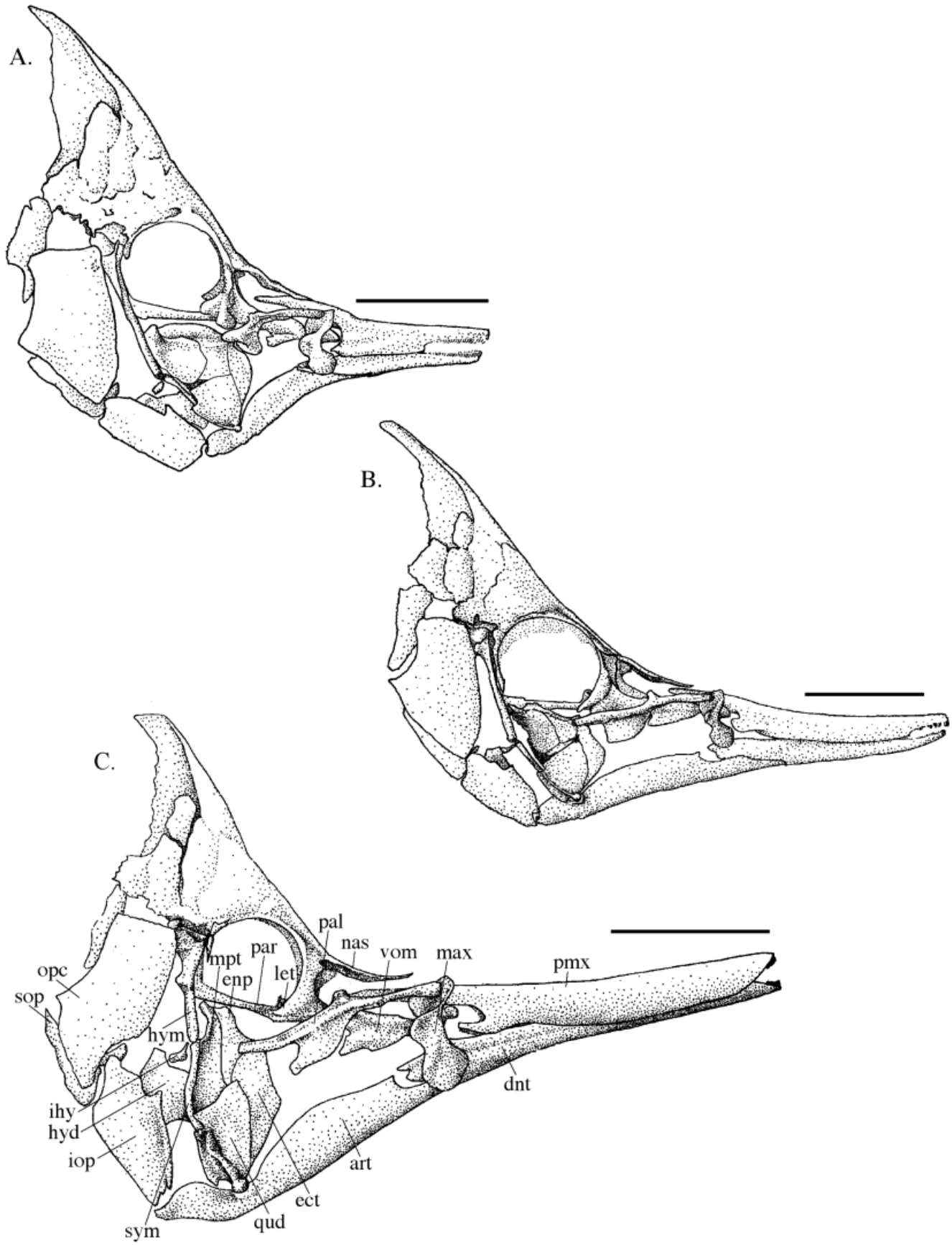

Fig. 5. Cranial anatomy of butterflyfishes drawn from cleared and stained specimens. **A**: *Chelmon rostratus*. **B**: *Forcipiger flavissimus*. **C**: *F. longirostris*. The orbital bones have been cut near the neurocranium and removed and the preopercle has been removed to facilitate a view of the suspensorial elements. opc, opercle; sop, subopercle; hym, hyomandibula; ihy, interhyal, hyd, hyoid; mtp, metapterygoid; enp, endopterygoid; ect, ectopterygoid; qud, quadrate; sym, symplectic; iop, interopercle; par, parietal; let, lateral ethmoid; pal, palatine; nas, nasal bone; vom, vomer; max, maxilla; pmx, premaxilla; art, articular; dnt, dentary (articular + dentary = mandible or lower jaw). Scale bars are 1.0 cm.

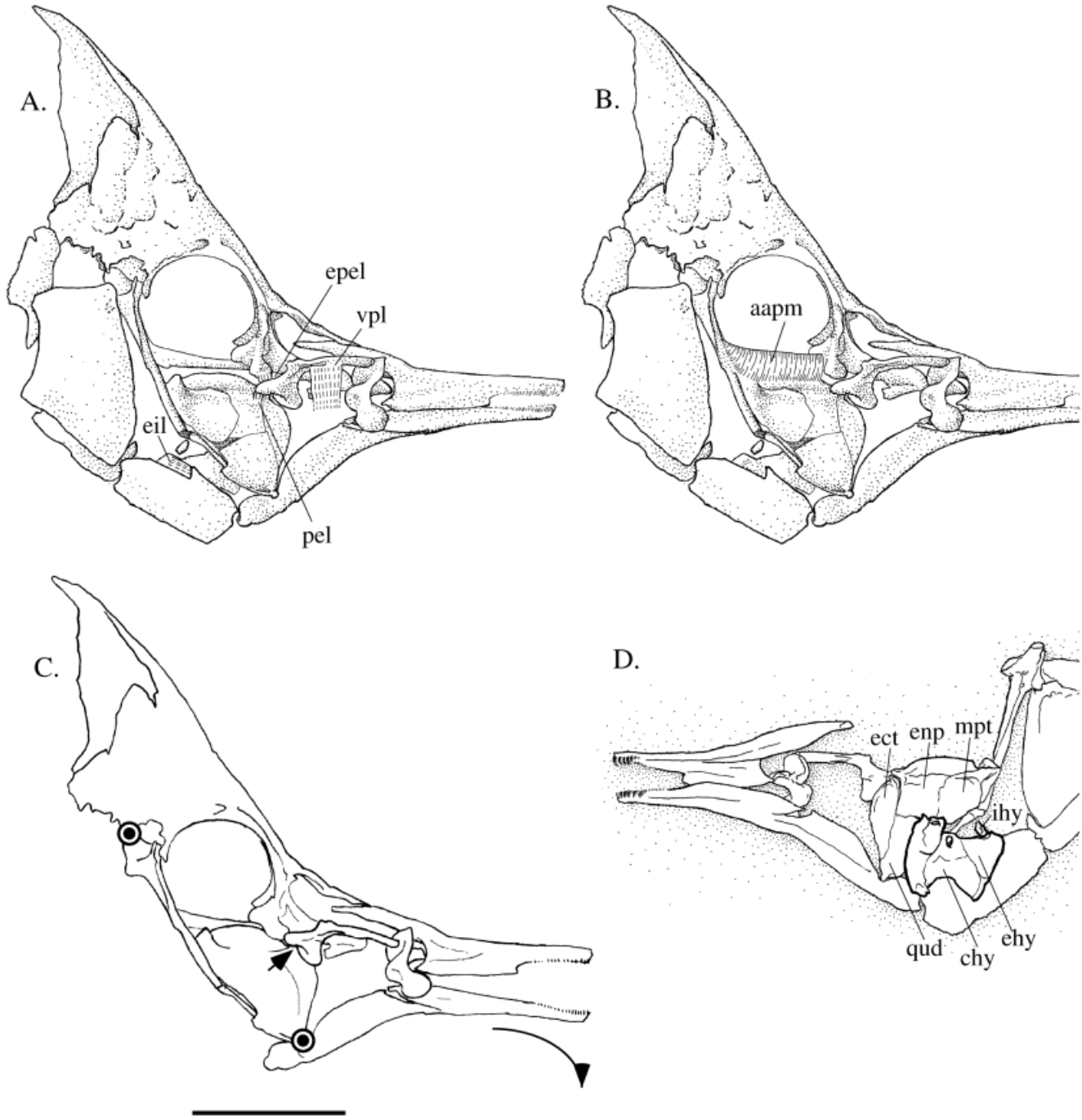

Fig. 6. Specific aspects of the cranial anatomy of *Chelmon rostratus*. **A**: Ligaments associated with the suspensorium. **B**: The superficial portion of the adductor arcus palatini muscle. **C**: Reduced cranial morphology illustrating jaw motion when two joints are present, one within the suspensorium (note that the joint between the palatine and the quadrate complex is a sliding joint). **D**: Reduced cranial morphology showing a medial view of the hyoid apparatus on the same side of the head (note that stippling has been used to enhance the sections where bones are not present). eil, epihyal-interopercular ligament; epel, modified ethmopalatoendopterygoid ligament; pel, palatoendopterygoid ligament; vpl, vomeropalatine ligament; aapm, adductor arcus palatini muscle; ehy, epihyal; chy, ceratohyal (epihyal + ceratohyal = hyoid in Fig. 5); ihy, interhyal, ect, ectopterygoid; enp, endopterygoid; mtp, metapterygoid; qud, quadrate. In the mechanical drawing rotating joints are indicated by points and the direction of movement is indicated by arrows. Scale bars are 1.0 cm.

The cranial anatomy of *Johnrandallia* and *Heniochus* is similar. In all *Johnrandallia* and *Heniochus* examined, the suspensorium is unmodified relative to *Chaetodon* (Fig. 3). There is no evidence of palatine movement in manipulated specimens and a distinct palatoendopterygoid ligament appears to be

absent. The ethmopalatoendopterygoid ligament is robust and is in two parts, as found in *Chaetodon* (Fig. 4). The palatine and endopterygoid bones are like *Chaetodon*. A distinct vertical vomeropalatine ligament is present. Also like *Chaetodon*, there is no evidence of a mobile posterior joint on the suspensorium. The quadrate complex did not rotate anteriorly during manipulation of the jaw in cleared and stained specimens. During jaw protrusion the lower jaw tip rotated ventrally on the quadrate while the premaxilla protruded anteriorly.

The suspensorial bones of *Forcipiger flavissimus* are reduced relative to *Chaetodon* and are similar in mobility to *Chelmon rostratus* (Fig. 5). The suspensorium of *F. flavissimus* exhibits not one joint, like *Chel. rostratus*, but two joints. The first of these is functionally similar to *Chel. rostratus* and is located anteriorly between the palatine and endopterygoid. The endopterygoid and metapterygoid bones are reduced anteriorly and the palatine is elongate and extends posteriorly to articulate on its medial surface with the lateral surface of the endopterygoid at the confluence of the endo- and ectopterygoid bones. A simple rotating joint is formed there by the palatoendopterygoid ligament, a ligament also found in *Chel. rostratus*. There is another robust ligament that extends from the ventral medial surface of the lateral ethmoid on the neurocranium to the dorsal lateral surface of the endopterygoid process. This ligament may be a modification of the ethmopalatoendopterygoid ligament; however, it is a different modification from that found in *Chel. rostratus*, where only the portion that extends from the lateral ethmoid to the palatine is present. In *F. flavissimus* this ligament appears to restrict motion of the palatine on the neurocranium relative to *F. longirostris* (see description of *F. longirostris*). A distinct vertical vomeropalatine ligament is also present that is like *Chaetodon* in its configuration. The second joint within the suspensorium is a posterior joint, like *Chel. rostratus*; however, this joint is between the hyomandibula and the symplectic. The hyomandibula lacks a solid articulation with the symplectic or the quadrate but is connected to them via soft tissue. Therefore, the hyomandibula does not move when the jaw is protruded in manipulated specimens. The quadrate, symplectic, endo-, ecto-, and metapterygoid form a complex that rotates at a dorsal-medial process of the metapterygoid. An angle of about 10° is formed between the hyomandibula and symplectic as the lower jaw is protruded, rather than depressed, in manipulated cleared and stained specimens.

Cleared and stained specimen examination revealed that the cranial bones of *Forcipiger longirostris* appear the most anatomically extreme relative to *Chaetodon xanthurus* (Fig. 5), particularly in the suspensorium and jaws. The suspensorium of *F. longirostris* exhibits the same two joints found in *F. flavissimus*. The first of these is the anterior joint between the palatine and endopterygoid. However, the endopterygoid and metapterygoid bones of *F. longirostris* are more reduced anteriorly relative to *F. flavissimus*. The palatine is elongate and extends posteriorly to articulate on its medial surface with the lateral surface of the endopterygoid at the confluence of the endo- and ectopterygoid bones. A joint is formed by the palatoendopterygoid ligament that can rotate a much greater degree than seen in *F. flavissimus,* due to the reduction of the endopterygoid and metapterygoid bones (Fig. 7). There is also a vertical vomeropalatine ligament that extends from the anterior process of the palatine ventrally to the lateral surface of the vomer (Fig. 7). The presence and configuration of this ligament is similar to *Chaetodon*, but in *F. longirostris* the ligament appears to limit anterior motion of the palatine. The second joint is located posteriorly and occurs at the interface of the hyomandibula and quadrate–symplectic complex (Fig. 7), as in *F. flavissimus*. The quadrate, symplectic, endo-, ecto-, and metapterygoid form an anteroposteriorly compressed unit that rotates at a dorsal-medial process of the metapterygoid as the lower jaw is protruded in manipulated specimens. This joint could freely rotate as much as 25° in manipulated *F. longirostris* specimens, resulting in extensive anterior movement of the jaw joint (quadrate-articular), and thus the lower jaw.

Examination of preserved specimens revealed a modification of the adductor arcus palatini (AAP) muscle primarily in *Forcipiger longirostris* (Fig. 7). The AAP originates along the basisphenoid and inserts onto the metapterygoid, endopterygoid, and ectopterygoid bones. In most perciforms, and the short-jawed butterflyfishes, the fibers are oriented medial-laterally (Motta, 1982; Fig. 4B). In all *Heniochus, Johnrandallia, Chelmon,* and *Prognathodes*, like the *Chaetodon* studied, the fibers of the AAP are oriented medial-laterally. In *F. longirostris* the anterior third of the muscle originates from the anterior-ventral region of the orbit, mostly from the ethmoid bar. This portion of the AAP is considerably thicker than the posterior region. The endo- and ectopterygoid bones, as indicated above, are reduced and most of the fibers of the AAP extend posteriorly, rather than laterally, to insert on the metapterygoid (behind the orbit). A few fibers of the AAP insert on the hyomandibula (not shown in Fig. 4B). In *F. flavissimus* there is a slight shift in fiber orientation in the anterior portion of the muscle, but not to the degree seen in *F. longirostris*. This slight shift is achieved by an extension of the dorsal margin of the endopterygoid bone that effectively extends the attachment site of the AAP dorsolaterally (Fig. 7).

Linkage Models

Our anatomical observations suggested that up to three distinct joints may be involved in lower jaw motion, two of which are novel and derived within

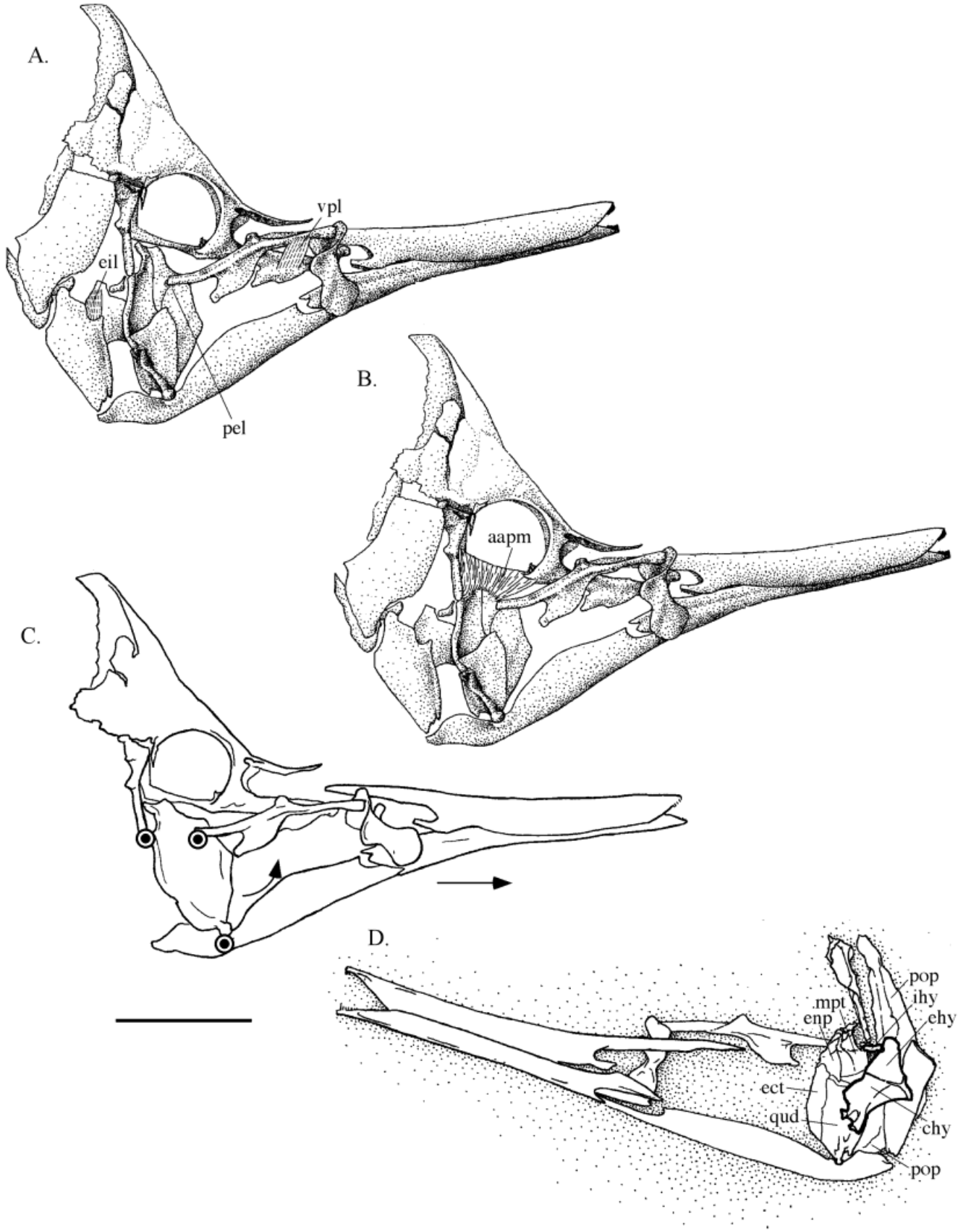

Figure 7

the Chaetodontidae. Depending on the number of joints present, there are different consequences for the path of motion of the lower jaw. *Chaetodon xanthurus* is used to demonstrate the condition found in all of the short-jawed butterflyfishes we studied, including *Prognathodes, Heniochus,* and *Johnrandallia* (Fig. 4C). This condition is also found in generalized perciforms. The suspensorial bones are fixed such that there is no rotation during jaw depression and no movement of the jaw joint. The lower jaw rotates on the fixed quadrate and the jaw rotates ventrally through an arc.

Chelmon rostratus is diagramed with intermediate modifications (Fig. 6C). The hyomandibula moves with the quadrate complex; thus, a posterior point of limited rotation is at the articulation of the hyomandibula with the skull. The quadrate complex slides under the palatine due to the loose articulation between the two. The palatine itself is largely fixed, but slight movement of the quadrate relative to the palatine provides the freedom necessary for the quadrate to rotate a small amount on the lower jaw during depression; thus, the lower jaw moves both anteriorly and ventrally.

Forcipiger longirostris is used to illustrate the condition in both *Forcipiger* sp. There is a total of three joints, two in the suspensorium and one at the quadrate-articular jaw joint. Two suspensorial joints facilitate rotation relative to the fixed neurocranium (Fig. 7C). The rotating quadrate complex is shown pivoting on the hyomandibula and the palatine. Anterior rotation of the quadrate facilitates anterior motion of the jaw joint, and therefore protrusion of the lower jaw. If rotation occurs simultaneously at the hyomandibula-metapterygoid joint and the quadrate-lower jaw joint, the lower jaw will follow an anterior course, with little dorsal or ventral motion. *Forcipiger flavissimus* exhibits a less mobile version of this model than *F. longirostris*, due to the constraints outlined in the previous section.

Fig. 7. Aspects of the cranial anatomy of *Forcipiger longirostris.* **A**: Ligaments associated with the suspensorium. **B**: The superficial portion of the adductor arcus palatini muscle. **C**: Reduced cranial morphology illustrating jaw motion when three joints are present, two within the suspensorium. **D**: Reduced cranial morphology showing a medial view of the hyoid apparatus also on the right side of the head (note that stippling has been used to enhance the sections where bones are not present). vpl, vomeropalatine ligament; pel, palatoendopterygoid ligament; eil, epihyal-interopercular ligament; aapm, adductor arcus palatini muscle; ehy, epihyal; chy, ceratohyal (epihyal + ceratohyal = hyoid in Fig. 5); ihy, interhyal, ect, ectopterygoid; enp, endopterygoid; mtp, metapterygoid; qud, quadrate; pop, preopercle (not shown in other drawings). Note the compressed pterygoid elements, the dorsoventrally oriented interopercle, and the anterior-posterior oriented adductor arcus palatini muscle fibers. In the mechanical drawing rotating joints are indicated by points and the direction of movement is indicated by arrows. Scale bars are 1.0 cm.

Kinematic Analysis

The five species in the kinematic analysis differed only slightly in the general behaviors related to prey capture. In each capture event the individual would swim around the aquarium searching for a prey item. Detection of a prey item was indicated by a direct approach towards the brine shrimp and then braking, using the pectoral fins, generally with the anterior tip of the jaws within about a centimeter of the prey item. Although some forward locomotion continued due to inertia, the strike was initiated with the onset of lower jaw protrusion or depression (Fig. 8; t_0 in sequences A–E). Peak jaw protrusion or depression was achieved at 20–28 ms in each species (Fig. 8), after which the jaws would return to their relaxed, prefeeding position. Failed attempts at prey capture occurred only in the *Forcipiger* species and *Chelmon rostratus*, and were generally followed quickly by additional attempts at the same individual brine shrimp.

Subtle differences existed in the relative contribution of rotation of the preopercle during jaw rotation and protrusion (Fig. 9). *Forcipiger longirostris* showed the greatest angular excursion of the lower jaw on the preopercle, achieving angles upwards of 20°. However, this was not significantly greater than the maximum angles achieved by the other species, which ranged from 15–18° (Fig. 9; $F_{4,57} = 1.41$, $P = 0.244$, power = 0.40). *Forcipiger longirostris* exhibited a uniquely large change in the angle of the preopercle with the neurocranium, achieving average maxima of around 12° (Fig. 9; $F_{4,57} = 129.11$, $P < 0.0001$, Fisher's PLSD all $P < 0.0001$). *Forcipiger flavissimus* achieved about 7°, which was larger than the average maxima achieved by *Chelmon rostratus*, about 4° (Fisher's PLSD $P < 0.0001$). This small amount of rotation in *Chel. rostratus* was significantly greater than in the two short-jawed species (Fisher's PLSD $P < 0.0001$), which did not rotate the preopercle relative to the neurocranium.

The path of motion of the lower jaw, produced by the rotating preopercle and depression of the lower jaw, was mostly anterior in *Forcipiger longirostris* (Fig. 10). Lower jaw movement was also anteriorly directed but protruded to a significantly smaller maxima in *F. flavissimus* (Fig. 10; $F_{4,57} = 22.63$, $P < 0.0001$, Fisher's PLSD $P < 0.0001$). There was a much stronger component of ventrally directed movement in *Chelmon rostratus*; however, the amount of anterior protrusion was not significantly different from *F. longirostris* (Fisher's PLSD $P = 0.111$) and was significantly greater than *F. flavissimus* (Fisher's PLSD $P < 0.0001$). *Forcipiger flavissimus* did exhibit more anterior protrusion of the lower jaw than *Chaetodon xanthurus* (Fisher's PLSD $P = 0.095$), which did not differ from *Heniochus acuminatus* (Fisher's PLSD $P = 0.034$). Almost purely ventrally directed movement was exhibited by *C. xanthurus* and *H. acuminatus* (Fig. 10).

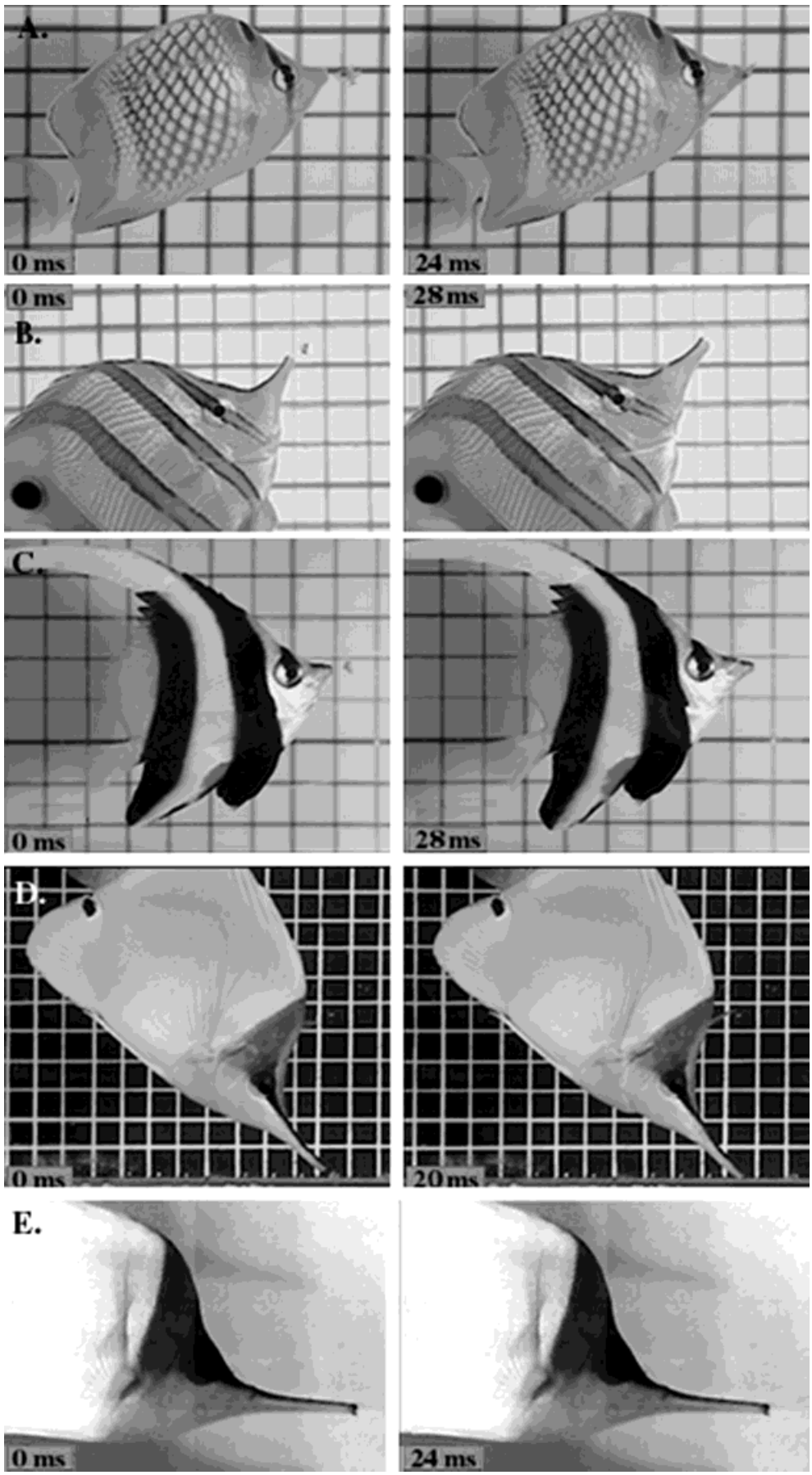

Fig. 8. High-speed video frames of individuals at t_0 (left) and at peak jaw protrusion (right). The time of peak jaw protrusion is noted in each frame. Species are: (**A**) *Chaetodon xanthurus*, (**B**) *Chelmon rostratus*, (**C**) *Heniochus acuminatus*, (**D**) *Forcipiger flavissimus*, and (**E**) *F. longirostris*. All events shown are successful prey captures. The brine shrimp is still visible in the jaws of *C. xanthurus* at peak protrusion. The grids in images **B–E** are 1.0 cm^2.

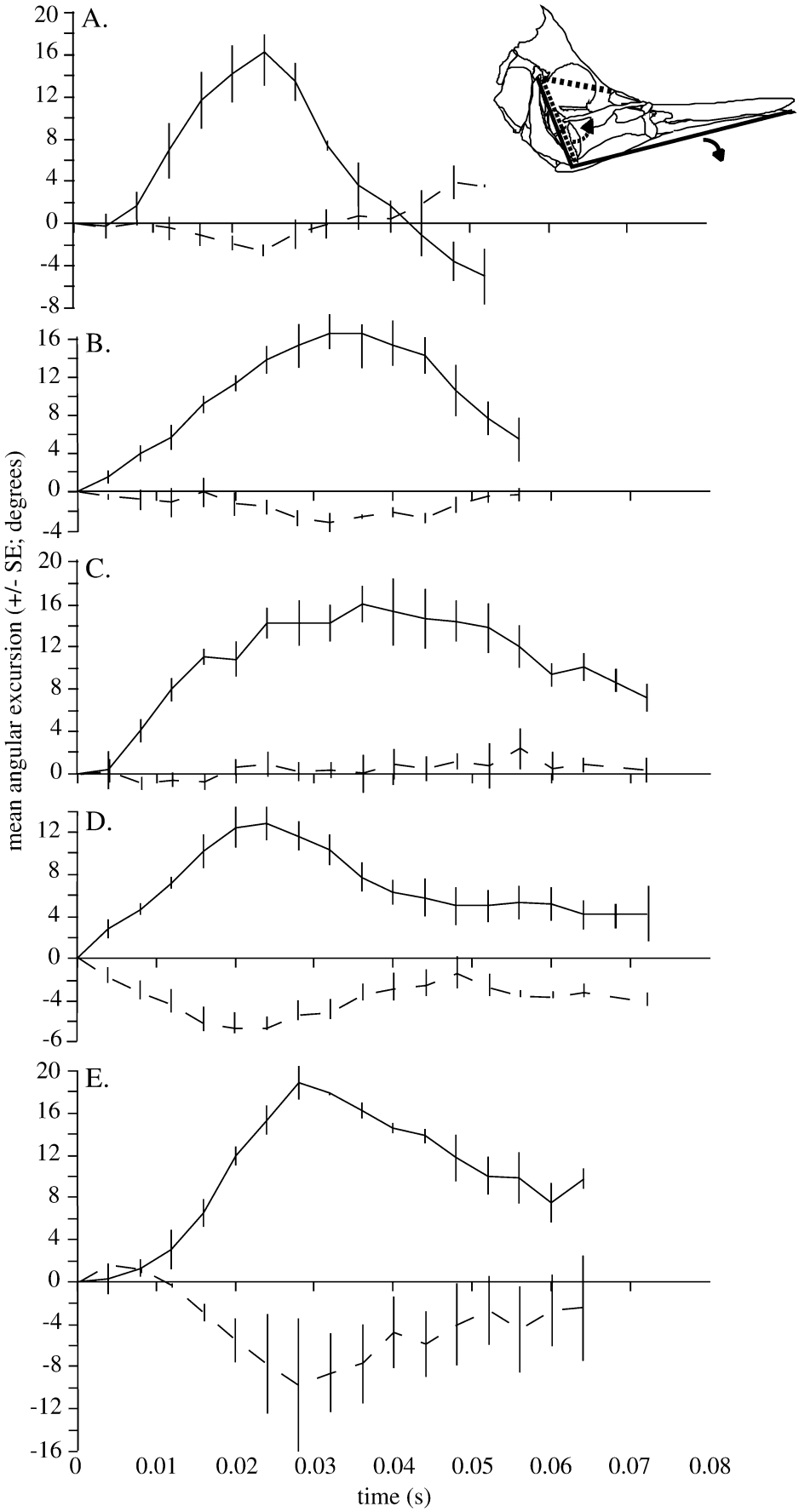

Fig. 9. The angle of the preopercle with the lower jaw (solid lines) and with the neurocranium (dashed lines) for: (**A**) *Chaetodon xanthurus*, (**B**) *Chelmon rostratus*, (**C**) *Heniochus acuminatus*, (**D**) *Forcipiger flavissimus*, and (**E**) *F. longirostris*. The angles, expressed in degrees, are shown along with the path of motion of the mobile components on a skull of *F. longirostris* for reference. Note that the angle of the preopercle with the neurocranium is expressed as a negative excursion (see Fig. 2C; angle b). If it changes during prey capture, this angle is reduced relative to a relaxed position at t_0, while the angle of the preopercle with the lower jaw is increased during feeding (Fig. 2C; angle c). In expressing angular excursions the starting value has been standardized to zero (prior to estimation of means) and all movements are relative to a value of zero at t_0. For each species the four strikes per individual were averaged and then an overall mean calculated from those individual means. For clarity, data from species that were analyzed at 500 frames sec^{-1} have been subsampled so that all data shown are at 250 frames sec^{-1}.

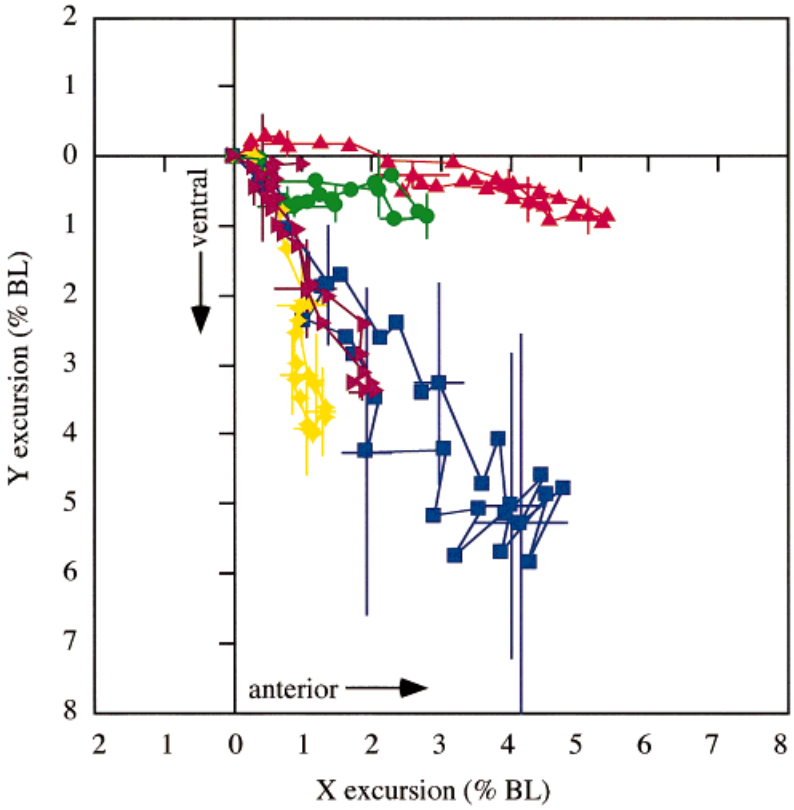

Fig. 10. Mean path of the tip of the lower jaw as it is protruded during prey capture scaled relative to body length of the fish (%BL). The body length used to scale the data was the length from the anterior margin of the orbit to the tail tip; thus, jaw length is not included in the standardization procedure. Species are: (**A**) *Chaetodon xanthurus* (purple right facing triangles R), (**B**) *Heniochus acuminatus* (yellow diamonds F), (**C**) *Chelmon rostratus* (blue squares B), (**D**) *F. flavissimus* (green circles J), and (**E**) *Forcipiger longirostris* (red upright triangles H). The starting value for each path plot has been standardized to zero (prior to estimating means) and all movements are relative to a value of zero at t_0. The data were also rotated in coordinate space so that the fish body was parallel to the X-axis and anteroposterior movement of the lower jaw occurred along the X-axis. Values shown are the average of the four strikes per individual and then an overall mean calculated from those individual means. Error bars are SE; for graphical clarity only every fifth error bar is shown.

Cranial elevation was initiated at the same time as lower jaw protrusion or depression (i.e., t_0); however, the contribution of cranial elevation to the strike in each species was consistently small, with peaks between 4 and 5.5° (Fig. 11; $F_{4,57} = 0.86$, $P = 0.49$, power = 0.25). Maxilla rotation generally began by 10 ms into the strike and was much more variable among species. Rotation was significantly larger in *Forcipiger longirostris*, achieving a maximum of about 32° (Fig. 11; Fisher's PLSD all $P < 0.004$). Peak maxilla rotation occurred at approximately the same time as peak jaw protrusion or depression (see Fig. 9).

DISCUSSION

Our kinematic analysis of high-speed video footage revealed that *Forcipiger longirostris* can protrude its jaws in an anterior direction and to the greatest extent, while *F. flavissimus* protrudes its jaws anteriorly but to a shorter distance. *Chelmon rostratus* moves its jaws as much ventrally as anteriorly. *Heniochus acuminatus* and *Chaetodon xanthurus* exhibit an almost purely ventrally directed path of movement of the lower jaw, with only a slight amount of protrusion occurring because the lower jaw passes through an arc as it is depressed (Fig. 10). These kinematic patterns are consistent with the expectations of our mechanical diagrams.

With a single joint between the quadrate and the lower jaw, the tip of the lower jaw can only rotate ventrally. *Heniochus acuminatus* and *Chaetodon xanthurus* are unmodified from the generalized perciform condition in this respect and their jaw movements are constrained by a fixed suspensorium. Thus, in these species the lower jaw is depressed rather than protruded. If, however, there are two points of rotation, the second being the quadrate on the hyomandibula or the neurocranium, the lower jaw tip can potentially move anteriorly (see Fig. 7). The biomechanical models of *Forcipiger longirostris* and, to a large degree *F. flavissimus*, suggest that jaw protrusion can occur in a mostly anterior direction, facilitated by the novel joints within the suspensorium. *Chelmon rostratus,* with its more intermediate modifications, should have some anterior motion of the lower jaw, but the degree of that motion is limited and motion should occur secondarily in the ventral direction.

Mechanisms of Lower Jaw Protrusion

While the basic paths of movement are clear, the input motion that causes movement of the elongate jaws of these species has not been determined directly. Most lower vertebrates, including the short-jawed butterflyfish studied here (see also Motta, 1982), rely primarily on the action of the sternohyoideus muscle to depress the lower jaw through the mandibulo-hyoid coupling (Winterbottom, 1974; Motta et al., 1991; Lauder and Shaffer, 1993; for an exception see Wilga and Motta, 1998). In most te-

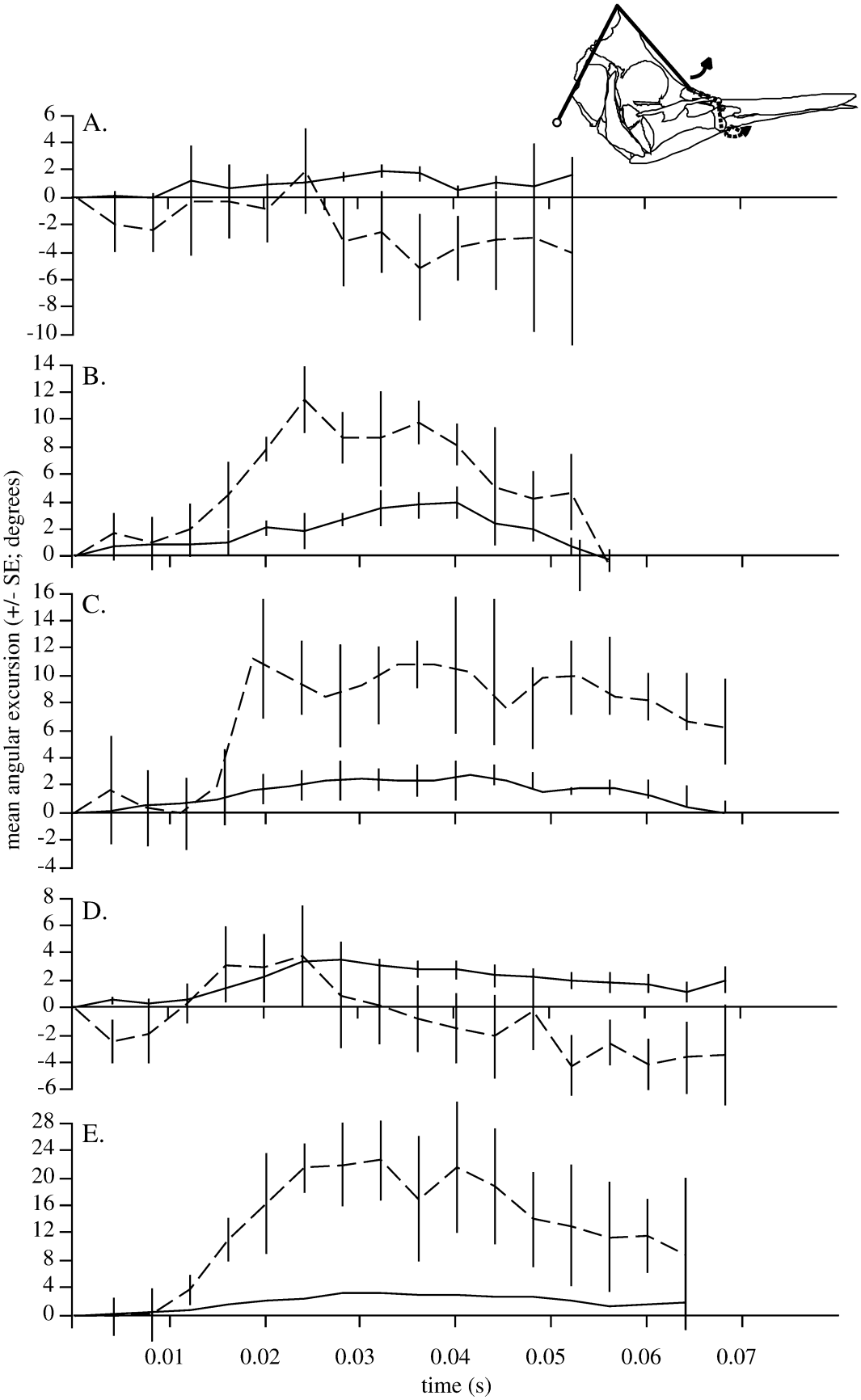

Fig. 11. Angular excursions of selected cranial elements during prey capture for: (**A**) *Chaetodon xanthurus,* (**B**) *Chelmon rostratus*, (**C**) *Heniochus acuminatus*, (**D**) *Forcipiger flavissimus*, and (**E**) *F. longirostris*. Angles are expressed as a change relative the angle at t_0. Change in cranial elevation is shown in solid lines and maxilla rotation in dashed lines. The angles are shown along with the path of motion of the mobile component on a skull of *F. longirostris* for reference (see Fig. 2C; angles a and d). In estimating angular excursions, the starting value has been standardized to zero (prior to estimation of means) and all movements are relative to a value of zero at t_0. Values shown are the average of the four strikes per individual and then an overall mean calculated from those individual means. Error bars are SE. All data shown are at 250 frames sec^{-1}.

leosts this muscle is located on the anterior-ventral surface of the pectoral girdle and runs forward to insert on the urohyal which attaches to the hyoid at the confluence of the left and right hyoid bars (Winterbottom, 1974). The pectoral girdle is held relatively immobile, or retracted a small amount by the action of the hypaxialis, so contraction of the sternohyoideus pulls the hyoid posteriorly. This force is transferred to the interopercle via the epihyal-interopercular ligament, which in turn puts tension on the interoperculomandibular ligament (see also Westneat, 1990). The small portion of the lower jaw located posterior to the jaw joint is pulled, causing the jaws to pivot on the fixed quadrate (see Fig. 5). The anterior tips of the lower jaw pass through an arc as they are depressed ventrally.

With respect to jaw motion in the long-jawed butterflyfishes this mechanism appears to present a paradox, as it would seem that sternohyoideus contraction could not protrude the lower jaws anteriorly instead of depressing them ventrally. However, our manipulations of cleared and stained specimens suggest a possible mechanism for sternohyoideus-powered jaw protrusion in *Forcipiger*. We found that pulling posteriorly on the urohyal, simulating input caused by the sternohyoideus (and hyoid depression), does result in forward protrusion of the lower jaws. This action is made possible by the modified orientation of the hyoid bar and the interopercle in *Forcipiger*. The hyoid and interopercle in *F. longirostris* are oriented mostly dorsoventrally rather than anteroposteriorly, as in more generalized taxa (see Fig. 7D). In both species of *Forcipiger* the epihyal-interopercular ligament is short and stout, oriented dorsoventrally, and attaches in a distinct notch of the interopercle (Fig. 7). Posteriorly directed force applied to the urohyal causes the hyoid bar to continue rotating about the interhyal, placing a dorsally directed tension on the epihyal-interopercular ligament (Fig. 7). As a result of the orientation of both the ligament and the interopercle bone, the anterior-ventral tip of the interopercle is rotated dorsally. This tends to push the quadrate dorsally into the skull, and because the quadrate complex is oriented somewhat anteriorly with respect to its joint on the hyomandibula (see Fig. 7), the quadrate-articular joint collapses anteriorly, rather than posteriorly. Anterior rotation of this joint causes anterior protrusion of the lower jaw.

The ability of *Forcipiger longirostris* to protrude the lower jaw anteriorly also appears to be facilitated by the position and fiber arrangement of the adductor arcus palatini muscle (see Fig. 7B). The change in fiber orientation from medial-lateral to anteroposterior appears to allow the adductor arcus palatini to rotate the pterygoid-quadrate-symplectic complex dorsally (Fig. 7B). Thus, the quadrate complex rotates at the base of the hyomandibula. As the quadrate complex is rotated, the joint between the quadrate and the lower jaw is also rotated dorsally and anteriorly, facilitating lower jaw protrusion during prey capture.

The function of the adductor arcus palatini during prey capture has not been experimentally measured in butterflyfishes. However, if we are correct that the AAP generates the input force used for protruding the lower jaw, a concomitant change in muscle activity pattern from the generalized perciform condition must have occurred in *Forcipiger*. The AAP is usually an adductor of the suspensorium, active during the preparatory and compressive phases of prey capture (Liem, 1980; Lauder, 1983). Muscle stimulation experiments suggest that this adductor function of the AAP is probably conserved in *Chaetodon* (Motta, 1982). In *Forcipiger longirostris*, however, the lower jaws are protruded prior to and during actual prey entrainment. Thus, under our hypothesis, the AAP must be activated during the expansive phase of feeding (between the preparatory and the compressive phases) if the AAP is involved in jaw protrusion. Thus, we predict that the AAP has a novel period of activation in *F. longirostris*. The AAP cannot be simultaneously responsible for both suspensorial adduction and jaw protrusion—the two activities are antagonistic. Other muscles typically active with the AAP to adduct the suspensorium, such as the adductor mandibulae (Lauder, 1983), may well be sufficient to adduct the suspensorium of *F. longirostris* in the absence of AAP activity.

Modifications to the AAP in the taxa studied here may have arisen as an indirect consequence of modifications to the suspensorium. In *Forcipiger longirostris*, the attachment site of the AAP, the endo- and ectopterygoid bones, are reduced and positioned posteriorly relative to the other butterflyfish taxa studied. This has the effect of causing the fibers of the AAP to extend posteriorly, rather than laterally, and results in a shift in fiber orientation without modifying the origin and insertion of the muscle. In both *F. flavissimus* and *Chelmon rostratus*, a mostly unmodified (i.e., medial-laterally oriented fibers) AAP could still act to facilitate some rotation of the quadrate complex. The quadrate complex in these two species is large and plate-like and pulling dorsally on it, where the AAP attaches, can move the quadrate dorsally, causing the joint between the lower jaw and the quadrate to also be translated dorsally and the jaw to be protruded anteriorly. In other chaetodontids the fixed quadrate prevents this motion.

Comparisons with the only other studied species that exhibits anteriorly directed lower jaw protrusion suggest a central importance of the rotating quadrate for such jaw protrusion. In the sling-jaw wrasse, *Epibulus insidiator* (Labridae), protrusion of the lower jaw is also achieved by the addition of a joint in the suspensorium (Westneat and Wainwright, 1989). A novel ligament, the vomerointeropercular ligament, transmits the motion of cranial elevation to the interopercle bone (Westneat, 1991). Rotation of the interopercle places tension on the

interopercular-mandibular ligament, placing a force at the posterior end of the lower jaw. If the quadrate were fixed, this force would cause the lower jaw to rotate around the quadrate-lower jaw joint and the jaw would be depressed, as in the generalized perciform condition. The quadrate, however, rotates in parallel with the interopercle and the force is transferred into anteriorly directed movement of the lower jaw (Westneat, 1991).

Thus, the mechanism that powers quadrate rotation differs in *Forcipiger* and *Epibulus*. Modifications to the motion of the hyoid apparatus and to the AAP in *Forcipiger* have the function of cranial rotation in *Epibulus* in rotating the quadrate. However, the interopercle clearly rotates in *F. longirostris* during jaw protrusion and a sternohyoideus mechanism has been identified, linking interopercle rotation to lower jaw protrusion directly. The contribution of interopercle movement combined with a rotating quadrate appears to be consistent between *Forcipiger* and *Epibulus*. It is the addition of a rotating quadrate, achieved by any means, that adds an "unfolding" section to the lower jaw and is the common feature in this convergence in function.

Evolution of Mobile Suspensoria and Elongate Jaws

Blum's (1988) phylogeny (Fig. 1A) is largely robust to our conservative character coding and subsequent analysis of 34 characters. Only three changes resulted from this first reanalysis. However, two of these changes are important for interpreting the evolution of the mobile suspensorium in the species with the longest jaws. These are the placement of *Forcipiger* as the outgroup to the three genera *Hemitaurichthys, Heniochus*, and *Johnrandallia*, and the tritomy of *Coradion* + *Chelmonops* (also long-jawed) + *Chelmon* for the *Chelmon* clade (Fig. 1B). Given this position of *Forcipiger*, the mobile suspensorium and length of the jaws may have been ancestral in the *Forcipiger* clade and lost within the *Hemitaurichthys* + *Heniochus* + *Johnrandallia* clade. Alternatively, the mobile suspensorium and long jaws could have arisen as a novel condition within *Forcipiger*. This possibility is even more likely if *Johnrandallia* is, in fact, the sister to the clade containing *Forcipiger* + *Heniochus* + *Hemitaurichthys* as the reduced character analysis suggested.

Separating these two alternatives also depends on the resolution of the polytomies present in the *Chelmon* clade and the mobility of the suspensorium of species within *Coradion* and *Chelmonops*. We can only assume that *Chelmonops* has a mobile suspensorium to accompany the elongate jaws that are like *Chelmon* in external appearance. If *Coradion* is the sister taxon to *Chelmonops* + *Chelmon*, then parsimony would suggest that the mobile suspensorium as well as long jaws evolved at least twice, once in the *Forcipiger* clade and again in the *Chelmon* clade. If, however, *Coradion* is the sister taxon to one of the other two genera, as suggested by Blum's phylogeny, then a long jaw plus mobile suspensorium could be the ancestral character for the seven taxa in this clade. These traits, then, would have been subsequently lost twice (Fig. 1A), once in *Coradion* and again in the *Hemitaurichthys* + *Heniochus* + *Johnrandallia* clade (potentially more if *Forcipiger* is not the outgroup to this clade). A single evolution of highly elongate jaws with a mobile suspensorium suggests the presence of an extant transformation series within the *Chelmon* + *Forcipiger* clade. Our reanalysis, however, finds no support for the necessary placement of *Coradion* (Fig. 1B). Resolving the *Chelmon* polytomy will be an important step for future research.

Despite having slightly elongate jaws, *Prognathodes* is anatomically undifferentiated from *Chaetodon* in the suspensorial region (see also Blum, 1988). Thus, we found no evidence of a mobile suspensorium and an anteriorly protruding jaw within the large *Chaetodon* branch of the phylogenetic tree (Fig. 1B). The small number of characters used in generating the phylogenies, however, suggests that relationships may change if a more extensive dataset is used. Currently the node between *Chaetodon* and *Prognathodes* is poorly supported. Additional phylogenetic analyses may find that *Prognathodes* is more appropriately placed at the base of the long-snouted clade, filling in a possible transition between a short-jawed ancestor and *Chelmon rostratus*. It is equally viable given the existing information that *Prognathodes* represents an independent evolution of modified jaws without concomitant changes to the suspensorium.

Heniochus and *Johnrandallia* are also morphologically similar to *Chaetodon*. Functionally, *H. acuminatus* shares the same immobile suspensorial elements with *C. xanthurus* and both exhibit jaw depression in the manner of a generalized perciform. However, the placement of *Heniochus* and *Johnrandallia* within the *Forcipiger* clade is one of the best-supported nodes on the tree. This suggests that the anatomical similarity between *Chaetodon* and *Heniochus* + *Johnrandallia* either represents a retained ancestral morphology or a morphology that *Heniochus* + *Johnrandallia* secondarily evolved from a long-jawed ancestor and structural constraints on the skeletal system facilitate their looking and functioning much like *Chaetodon*. Given that the current phylogenetic evidence more strongly supports the notion that elongate jaws and mobile suspensoria evolved independently in *Chelmon* and *Forcipiger*, it is more likely that *Heniochus* and *Johnrandallia* have retained an ancestral morphology.

Overall, we found that the longest-jawed species, *Forcipiger longirostris*, possesses both structural and muscular novelties that affect the kinematics of

the species and facilitate a novel pattern of movement, anterior protrusion of the lower jaw. The two butterflyfish species with the moderately elongate jaws lack extreme modification and cannot protrude their jaws as far (in the case of *F. flavissimus*) or as purely anteriorly (in the case of *Chelmon rostratus*). *Forcipiger* and *Chelmon* also possess slightly different solutions to the problem of creating movement within the suspensorium. Combined with their positions on the phylogeny, this suggests that this type of change, where the suspensorium is "freed-up," could have occurred more than once in the family. Further understanding of the evolutionary transformation to anteriorly directed jaw protrusion and a mobile suspensorium will depend ultimately on the resolution of phylogenetic relationships and further kinematic analyses and detailed morphological study of additional members of the Chaetodontidae.

ACKNOWLEDGMENTS

The authors thank J. Grubich, A. Carroll, and D. Bolnick, as well as two reviewers, for helpful feedback on the manuscript. P. Motta offered valuable anatomical insights and I. Hart expertly completed the anatomical drawings. M. Foster, J. Grubich, and A. Carroll assisted with collecting video data for several species at UCD. We thank River City Aquatics and Capitol Aquarium (Sacramento, CA, USA), Quality Marine Tropicals (Los Angeles, CA, USA), B. Squire of Cairns Marine Aquarium Fish (Cairns, Australia), R. Tunin, and T. Waltzek for their cooperation and assistance in locating specimens. F. Nosratpour and the Birch Aquarium (University of California San Diego, La Jolla, CA, USA) provided some particularly hard to locate specimens. R. Tunin's knowledge and assistance with butterflyfish husbandry was most helpful. The Adaptive Optics video system used in Australia was purchased under NSF grant IBN-9306672 to PCW, and this research was supported by a grant from the Australian Research Council to DRB and PCW, and by an NSF pre-doctoral fellowship to CDH.

LITERATURE CITED

Alexander RMcN. 1967. Mechanisms of the jaws of some atheriniform fish. J Zool Lond 151:233–255.

Allen GR, Steene R, Allen M. 1998. A guide to angelfishes and butterflyfishes. Perth, Western Australia: Odyssey Publishing, Vanguard Press. p 250.

Blum SD. 1988. Osteology and phylogeny of the Chaetodontidae (Pisces: Perciformes). Ph.D. Dissertation. University of Hawaii, Honolulu.

Cox EF. 1994. Resource use by corallivorous butterflyfishes (Family Chaetodontidae) in Hawaii. Bull Mar Sci 54:535–545.

Dinkerhus G, Uhler LH. 1977. Enzyme clearing of Alcian blue stained whole vertebrates for demonstration of cartilage. Stain Technol 52:229–232.

Ferry-Graham LA, Wainwright PC, Bellwood DR. 2001. Prey capture in long-jawed butterflyfishes (Chaetodontidae): The functional basis of novel feeding habits. J Exp Mar Biol Ecol 256:167–184.

Harmelin-Vivien ML, Bouchon-Navarro Y. 1983. Feeding diets and significance of coral feeding among chaetodontid fishes in Moorea (French Polynesia). Coral Reefs 2:119–127.

Lauder GV. 1982. Patterns of evolution in the feeding mechanism of Actinopterygian fishes. Am Zool 22:275–285.

Lauder GV. 1983. Food capture. In: Webb PW, Weihs D, editors. Fish biomechanics. New York: Praeger Publishers. p 280–311.

Lauder G, Shaffer HB. 1993. Design of feeding systems in aquatic vertebrates: major patterns and their evolutionary interpretations. In: Hanken J, Hall BK, editors. The skull: functional and evolutionary mechanisms. Chicago: University of Chicago Press. p 113–149.

Liem KF. 1980. Adaptive significance of intra- and interspecific differences in the feeding repertoires of cichlid fishes. Am Zool 20:295–314.

Maddison WP. 1993. Missing data versus missing characters in phylogenetic analysis. Syst Biol 42:576–581.

Mayden RL, Wiley EO. 1992. The fundamentals of phylogenetic systematics. In: Mayden RL, editor. Systematics, historical ecology, and North American freshwater fishes. Stanford: Stanford University Press. p 114–185.

Motta PJ. 1982. Functional morphology of the head of the inertial suction feeding butterflyfish, *Chaetodon miliaris* (Perciformes, Chaetodontidae). J Morphol 174:174–283.

Motta PJ. 1984a. Mechanics and functions of jaw protrusion in teleost fishes: a review. Copeia 1–18.

Motta PJ. 1984b. Tooth attachment, replacement, and growth in butterflyfish, Chaetodon miliaris (Chaetodontidae, Perciformes). Can J Zool 62:183–189.

Motta PJ. 1985. Functional morphology of the head of Hawaiian and mid-Pacific butterflyfishes (Perciformes, Chaetodontidae). Env Biol Fish 13:253–276.

Motta PJ. 1988. Functional morphology of the feeding apparatus of ten species of Pacific butterflyfishes (Perciformes, Chaetodontidae): an ecomorphological approach. Env Biol Fish 22:39–67.

Motta PJ. 1989. Dentition patterns among Pacific and Western Atlantic butterflyfishes (Perciformes, Chaetodontidae): relationships to feeding ecology and evolutionary history. Env Biol Fish 25:159–170.

Motta PJ, Hueter RE, Tricas TC. 1991. An electromyographic analysis of the biting mechanism of the lemon shark, *Negaprion brevirostris*: functional and evolutionary implications. J Morphol 210:55–69.

Randall JE. 1985. Guide to Hawaiian reef fishes. Kaneohe, HI: Harrowood Books.

Randall JE, Allen GR, Steene RC. 1990. Fishes of the Great Barrier Reef and Coral Sea. Bathurst, Australia: Crawford House Press.

Sano M. 1989. Feeding habits of Japanese butterflyfishes (Chaetodontidae). Env Biol Fish 25:195–203.

Schaeffer B, Rosen DE. 1961. Major adaptive levels in the evolution of the Actinopterygian feeding mechanism. Am Zool 1:187–204.

Swofford DL. 1993. PAUP: phylogenetic analysis using parsimony, v. 3.1. Champaign: Illinois Natural History Survey.

Swofford DL, Maddison WP. 1992. Parsimony, character-state reconstructions, and evolutionary inferences. In: Mayden RL, editor. Systematics, historical ecology, and North American freshwater fishes. Stanford: Stanford University Press. p 186–224.

Tricas TC. 1989. Prey selection by coral-feeding butterflyfishes: strategies to maximize the profit. Env Biol Fish 25:171–185.

Westneat MW. 1990. Feeding mechanics of teleost fishes (Labridae; Perciformes): a test of four-bar linkage models. J Morphol 205:269–295.

Westneat MW. 1991. Linkage biomechanics and the evolution of the unique feeding mechanism of Epibulus insidiator (Labridae: Teleostei). J Exp Biol 159:165–184.

Westneat MW, Wainwright PC. 1989. Feeding mechanism of *Epibulus insidiator* (Labridae; Teleostei): evolution of a novel functional system. J Morphol 202:129–150.

Wilga CD, Motta PJ. 1998. Feeding mechanism of the Atlantic guitarfish *Rhinobatos lentiginosus*: modulation of kinematic and motor activity. J Exp Biol 201:3167–3184.

Winterbottom R. 1974. A descriptive synonymy of the striated muscles of the teleostei. Proc Acad Nat Sci Philadelphia 125: 225–317.

APPENDIX A

A list of the taxa Blum (1988) examined as either preserved specimens or radiographs to produce his character matrix. The names under the heading represent the taxa as traditionally assigned to genera and subgenera. The headings are the osteologically distinct taxa Blum designated and those used in our present analysis. All groups currently considered subgenera of the genus *Chaetodon* are preceded by a *C.* Finally, because the group defined as *C. Citharoedus* was ultimately identical in all character states to *C. Corallochaetodon,* only *C. Corallochaetodon* was used as an endpoint for these two groups in our analysis.

Amphichaetodon
- Amphichaetodon howensis
- Amphichaetodon melbae

Chelmon
- Chelmon marginalis
- Chelmon mulleri
- Chelmon rostratus

Chelmonops
- Chelmonops truncatus

Coradion
- Coradion chrysozonus
- Coradion altivelis

Forcipiger
- Forcipiger flavissimus

Hemitaurichthys
- Hemitaurichthys polylepis
- Hemitaurichthys thompsoni

Heniochus
- Heniochus chrysostomus
- Heniochus diphreutes
- Heniochus intermedius
- Heniochus varius

Parachaetodon
- Parachaetodon ocellatus

Johnrandallia
- Johnrandallia nigrirostris

Prognathodes
- Prognathodes aya
- Prognathodes guyotensis

C. Roa
- C. Roa excelsa

C. Roaops
- C. Roa burgessi
- C. Roa nippon
- C. Roa tinkeri

C. Exornator
- C. Rhombochaetodon argentatus
- C. Rhombochaetodon madagascariensis
- C. Rhombochaetodon mertensii
- C. Rhombochaetodon xanthurus
- C. Chaetodon miliaris
- C. Chaetodon multicinctus
- C. Chaetodon blackburnii
- C. Chaetodon citrinellus
- C. Chaetodon daedalma
- C. Chaetodon dolosus
- C. Chaetodon fremblii
- C. Chaetodon guentheri
- C. Chaetodon guttatissimus
- C. Chaetodon punctatofasciatus
- C. Chaetodon quadrimaculatus
- C. Chaetodon sanctaehelenae

C. Megaoprotodon
- C. Megaprotodon trifascialis

C. Gonochaetodon
- C. Gonochaetodon baronessa
- C. Gonochaetodon larvatus
- C. Gonochaetodon triangulum

C. Tetrachaetodon
- C. Tetrachaetodon bennetti
- C. Tetrachaetodon plebeius
- C. Tetrachaetodon speculum
- C. Tetrachaetodon zanzibariensis

C. Corallochaetodon
- C. Corallochaetodon austriacus
- C. Corallochaetodon melapterus
- C. Corallochaetodon trifasciatus
- C. Citharoedus meyeri
- C. Citharoedus ornatissimus
- C. Citharoedus reticulatus

C. Rabdophorus
- C. Chaetodontops adiergastos
- C. Chaetodontops collare
- C. Chaetodontops fasciatus
- C. Chaetodontops flavirostris
- C. Chaetodontops lunula
- C. Chaetodontops semilarvatus
- C. Chaetodontops weibeli
- C. Rabdophorus auriga
- C. Rabdophorus ephippium
- C. Rabdophorus falcula
- C. Chaetodon melannotus
- C. Chaetodon ocellicaudus
- C. Rabdophorus gardineri
- C. Rabdophorus lineolatus
- C. Rabdophorus mesoleucos
- C. Rabdophorus nigropunctatus
- C. Rabdophorus rafflesi
- C. Rabdophorus selene
- C. Rabdophorus semeion
- C. Rabdophorus ulientensis
- C. Rabdophorus vagabundus

C. Lepidochaetodon
- C. Chaetodon kleinii
- C. Chaetodon trichrous
- C. Lepidochaetodon unimaculatus

C. Discochaetodon
- C. Discochaetodon aureofasicatus
- C. Discochaetodon octofasciatus
- C. Discochaetodon rainfordi
- C. Discochaetodon tricinctus

C. Chaetodon
C. Chaetodon capistratus
C. Chaetodon hoefleri
C. Chaetodon ocellatus
C. Chaetodon pelewensis
C. Chaetodon striatus

APPENDIX B

Characters and states used to construct phylogeny.

Character Matrix

	111111111122222222233333 123456789012345678901234567890123 *** * ** * **
E+S+A+D	00000000000000000000000000000000
Pomacanthidae	00000000000000000000100001002000000
Amphichaetodon	11100002010000100011001010000001111
Chelmonops	12100002110121211101002010000001111
Chelmon	12100002110121311101002010000001111
Coradion	12100002110121311101102010000001111
Forcipiger	11101001011111811011102010000010111
Hemitaurichthys	11101001010131411011002110100101111
Heniochus	11100001010131411011002110100101111
Johnrandallia	11100001010131111001002110100101111
Prognathodes	11110002000041110101103011100000111
C. Roa	11110002000041100001103011000000111
C. Chaetodon	13110102000041100100103011011001111
C. Rabdophorus	23110102000041100100103011011001111
C. Roaops	34110102001041100100113011011001111
C. Exornator	34110102101041100100113011011001111
C. Lepidochaetodon	34110102101041120100113011011001111
Parachaetodon	25210212001041100200131011011011111
C. Megaprotodon	23210212001041510200111011011011111
C. Gonochaetodon	23110102001041520200111011011001111
C. Tetrachaetodon	23110102001041620200121001011001111
C. Discochaetodon	23110102001041510000121001011001111
C. Corallochaetodon	23110102001041710010123001011001111

Characters which were treated as ordered in Blum's (1988) phylogeny. E + S + A + D = Ephippidae, Scatophagidae, Acanthuridae, *Drepane*. Taxonomic units preceded by the initial *C.* are currently considered subgenera of *Chaetodon* rather than genera, as suggested by Blum (1988).

Character Descriptions (Modified from Blum, 1988)

1. First dorsal pterygiophore. (0) Simple, no buttresses or lateral processes. (1) First dorsal spine buttressed ventrally by lateral processes of the pterygiophore. (2) First dorsal pterygiophore with lateral processes anterior to erector dorsalis. (3) Fusion of lateral buttresses and anterior lateral process to surround erector dorsalis.
2. Predorsal bones. (0) No sequential articulation between first dorsal pterygiophore, predorsal bones, and supraoccipital crest. (1) Sequential articulation between supraoccipital, predorsal bones, and first dorsal pterygiophore. (2) First predorsal bone flattened and lacking posterior groove for second predorsal bone. (3) Single predorsal bone present. (4) Heads of predorsal bones thickened, but first retains posterodorsal groove. (5) Similar to character state 4 but lacks posterodorsal groove.
3. Pleural rib laminae. (0) Ribs with no anterior laminae. (1) Weakly developed laminae. (2) Well-developed laminae.
4. Lateral line. (0) Not truncate. (1) Truncate.
5. Lateral line scale count. (0) Less than 60. (1) More than 60.
6. Swimbladder. (0) With no anterior bilateral diverticulae. (1) With bulbous anterolateral diverticulae that attach to the supercleithral. (2) Swimbladder with narrow anterolateral diverticulae.
7. Swimbladder divided into anterior and posterior chambers. (0) No. (1) Yes.
8. Kidney morphology. (0) Kidney not extending beyond first hemal spine. (1) Kidney with posterior bilateral lobes. (2) Bilateral lobes fused around first hemal spine.
9. Branchiostegal rays reduced to five. (0) No. (1) Yes.
10. Basihyal large/keeled. (0) No. (1) Yes.
11. Hyoid artery foramen present in dorsal hypohyal. (0) Yes. (1) No.
12. Dorsal hypohyal thin and anterior surface faces laterally. (0) No. (1) Yes.
13. First epibranchial shape in anterior view. (0) Pomacanthidae shape. (1) Height and width equal, the axis is inclined medially, the dorsal cartilage is wide and protrudes above the dorsal margin, and the lateral cartilate is relatively tall. (2) The height to width ratio is 0.75, the axis inclined medially, and all of the pieces of cartilage are relatively small. (3) Height and width equal, the axis is horizontal, the medial cartilage is small, the dorsal and lateral cartilages are wide and tall. (4) Height to width ratio less than 1.0, the axis is declined medially, the medial cartilage is larger than in all other taxa, and the dorsal and lateral cartilages are of moderate size.
14. Third basibranchial broad and flat. (0) Yes. (1) No.
15. Jaw and tooth morphology. (0) Outgroup morphology. (1) The five to ten tooth rows are positioned such that there is almost always an overlap of tooth rows within each band. (2) Maximum number of rows per tooth band is 15, five bands of teeth in jaws, disorganized tooth arrangement, jaw teeth curved, produced more dorsoventrally. (3) Vertical orientation of the teeth, shortened teeth, more than three bands of tooth rows. (4) Teeth are short and straight, and less than three bands of tooth rows. (5) Jaw teeth straight and long, rows short, reduced overlap of rows. (6) All teeth on the descending premaxillary process absent. (7) Teeth of nearly equivalent length, coalesced into dense brush, number of bands is increased. (8) Long-jawed

but tooth rows oriented in the more common anteromedial to posterolateral direction, the alveoli are confined to the tip of the jaw, and three bands of tooth rows traverse the median symphysis.
16. Vomerine teeth. (0) Well developed. (1) Partially toothed. (2) Toothless.
17. Ethmoid foramen completely enclosed in the lateral ethmoid. (0) Yes. (1) No.
18. Mesethmoid structure. (0) Solid. (1) Sieve-like. (2) Lace-like.
19. Posterior mesethmoid extends beyond lateral ethmoids. (0) Yes. (1) No.
20. Vertical ridges present on the anterior mesethmoid. (0) No. (1) Yes.
21. Ethmomaxillary ligament present. (0) Yes. (1) No.
22. Palatopalatine ligament. (0) Originates on the medial face of the palatine's maxillary process. (1) Palato-palatine ligament moves posterodorsally, some fibers originating from small apophysis. (2) Apophysis well developed. (3) Originally coded as having state 1 in Blum's matrix (1988) but coded as unknown for character state 2.
23. Palato-vomerine ligament. (0) Two palato-vomerine ligaments not well separated. (1) Two palato-vomerine ligaments well separated. (2) Vertical palato-vomerine ligament inserts on maxillary process. (3) Apophysis present at insertion of vertical palato-vomerine ligament.
24. Basal section of the palatine is dorsoventrally narrow and almost rod-like. (0) No. (1) Yes.
25. Ectopterygoid wide. (0) No. (1) Yes.
26. Second circumorbital excluded from margin of orbit. (0) No. (1) Yes.
27. Third circumorbital with ventrally directed lamina. (0) No. (1) Yes.
28. Parietal reduced dorsoventrally. (0) No. (1) Yes.
29. Lateral escapular not enclosing temporal canal. (0) No. (1) Yes. (2) Lateral extrascapular enclosing only the parietal canal.
30. Medial extrascapular disc-like. (0) No. (1) Yes.
31. Posttemporal with large semicircular posterior laminae in adults. (0) No. (1) Yes.
32. Pleural ribs extending almost mid-ventral. (0) No. (1) Yes.
33. Basipterygio-postcleithral ligament present. (0) No. (1) Yes.
34. Anterior branchiostegal rays free. (0) No. (1) Yes.